Fluctuation, Relaxations, and Hydration in Liquid Water. Hydrogen-Bond Rearrangement Dynamics

Iwao Ohmine[*]

Institute for Molecular Science, Myodaiji, Okazaki, 444, Japan

Hideki Tanaka

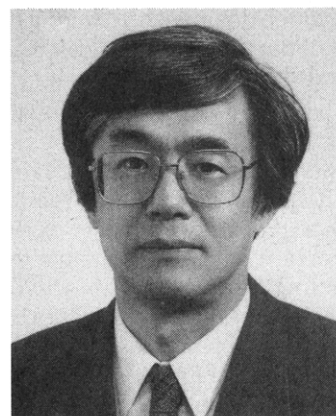*Department of Industrial Chemistry, Kyoto University, Yoshida, Sakyo-ku, Kyoto 606-01, Japan*

Contents

Iwao Ohmine received his B.S. from University of Tokyo and his Ph.D. from Harvard University. He did postdoctoral work at MIT and the Institute for Molecular Science, was a Research Associate at Keio University, and in 1982 joined Institute for Molecular Science, where he has been an Associated Professor of Department of Theoretical Studies. His research interests include electronic and dynamical aspects of photochemical reactions in gas and liquid and the dynamics of liquid and clusters.
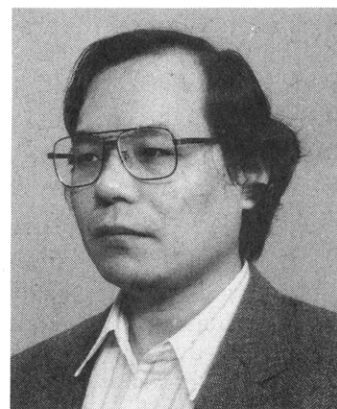
Hideki Tanaka was born in 1956. He received his Ph.D. degree from Kyoto University in 1984. He joined Ohmine's group at the Institute for Molecular Science. In 1987, he moved back to Kyoto University and is now an Instructor. His research interest has been focused on structure and dynamics of water and aqueous solutions and on the thermodynamic stability of hydrogen-bonded network systems such as clathrate hydrate.

I. Introduction

Water is the most ubiquitous substance on Earth, and it is known to have anomalous macroscopic and microscopic properties.[1,2] A decrease of viscosity with pressure, a large heat capacity and surface tension, density maximum at 4 °C, and an increase of rotational motion with pressure are a few of the properites. All these distinct microscopic and macroscopic properties of liquid water arise from the fact that water is a three-dimensional hydrogen-bonded network system. At low temperature, water exists in one of the ice crystalline structures. When the temperature increases to the melting point (0 °C), water absorbs the latent heat of about 80 cal/g, or 1.44 kcal/mol, hydrogen bonds are

partially broken and the system becomes "frustrated". The system then undergoes facile hydrogen-bond network rearrangement involving collective motions of many water molecules accompanied by large energy fluctuations.

In light of recent progress of experimental techniques that analyze relaxation dynamics of photochemical reactions in liquid, the liquid dynamics at the molecular level is becoming clarified and its theoretical interpretation is awaited. In this review we deal with liquid water dynamics in the time and spatial scales that relate to the fast chemical reactions in liquids, that is, a time scale in the order of sub to tens of picoseconds and at most tens of angstrom in spatial scale. In this frame, the explicit correlation of many molecules in structure and in dynamics is essential. In contrast, a conventional liquid theory, which deals with very long time and large spatial scale dynamics, emphasizes the diffusional aspect of liquid dynamics.

There have been many important reviews of structure and dynamics of liquid water. For example, an extensive review of studies up to early 1970s was given in the book by Eisenberg and Kauzmann.[1] Articles in *Water, a Comprehensive Treatise*[3] extensively cover the most important investigations up to early 1980s. Recent proceedings of workshops[4,5] and books[6] give an extensive overview of the current status of liquid water research. Among them, the works by Rice et al.,[2] Angell,[7] and Geiger et al.[8] are most related to the present review on theoretical aspects.

Theoretical models, which emphasize the order and disorder of the hydrogen bond network, have been proposed to explain the thermodynamic properties of liquid water. The flickering cluster model by Frank and Wen,[9] continuum model by Pople,[10] the random network model by Rice et al.,[2,11] and the percolation model by Stanley et al.[12,13] are the most typical ones. These models were quite successful in reproducing some liquid water anomalies. However the basic assumptions on which these models depend were not necessarily well founded and need to be carefully examined.

In spite of many existing models for the static properties of water, a model dealing with its dynamical properties has not been well established. The first molecular dynamics (MD) calculation on liquid water by Rahman and Stillinger[14] clarified many essential features of the dynamics as well as the structure of liquid water. From the analysis of their dynamical data, they concluded that some kinds of cooperative molecular motions are involved in liquid water. However, it has not been clarified what spatial, time, and energy scales cooperate in the dynamics. The main difficulty in dealing with liquid dynamics is how to extract core structural changes in dynamics (e.g., the fundamental change in the hydrogen bond network rearrangement in liquid water), which is buried in the thermal noise (i.e., vibrational movements). In their classic work,[15] Stillinger and Weber presented a new method to separate the fundamental structure component from the vibrational component (distortional displacements from the fundamental structures), to classify the dynamics, and to evaluate the thermodynamic quantities of liquid in terms of the fundamental structures. They regard multiple energy minima on a total potential energy surface as the fundamental structures and

termed those minima as inherent structures. The notion of separating the fundamental component from the vibrational component was also used in the earlier models, such as the bent hydrogen-bond model by Pople[10] and the random network model by Rice et al.[2,11] But a precise procedure to find the fundamental structures and use them in a dynamical analysis was first given by Stillinger and Weber.[15] Since then, many workers have investigated dynamical and thermodynamic properties of various cluster and liquid systems in terms of inherent structures. This was applied to analyze the cooperative nature of hydrogen-bond network in water dynamics and to show how the hydrogen-bond network rearrangement evolves in time.[16-19] Berry and co-workers[20] and Wales et al.[21] investigated the dynamics and structures of Ar atom cluster and molecular clusters by examining the potential energy surface involved. They constructed the thermodynamic functions, assuming harmonic form of each potential energy well, and predicted "melting" of finite clusters.[21b,22,23]

This review surveys the recent progress in the application of these theoretical and computational techniques to analyze strongly correlated molecular motions, collective motion, and fluctuation of hydrogen bond network in liquid water. As a problem bearing on the hydrogen-bond network structure and dynamics, we will discuss the hydration of nonpolar solutes. The physical origin of the hydrophobic hydration and the hydrophobic interaction is still controversial. Many theoretical methods such as the scaled particle theory, integral equation methods, and computer simulation technique have been proposed to calculate the hydration mixing energy, excess entropy, and solvent-induced solute–solute interaction. The recent development of these theoretical studies on hydration will be reviewed.

In section II, the previous models of liquid water are reviewed. Section III gives a brief sketch of MD calculation and water–water intermolecular interaction parameters. Inherent structures are introduced in section IV, and the fundamental structure changes with time, inherent structure transitions, are classified. Section V deals with multidimensional nature of the liquid water potential energy surface; normal modes and Raman experiment data are especially discussed. Long-time relaxation in liquid water dynamics is discussed in section VI. Dielectric relaxation and low-frequency Raman spectrum are examined. Section VII is given to review the recent advancement in the analysis of chemical reaction dynamics in liquid water. Theoretical development to deal with hydration is reviewed in section VIII. Conclusions are given in Section IX.

II. Models

The basic ideas of previous models for hydrogen-bond structures in liquid water are briefly reviewed here.

A. Mixture and Continuum Models

It is well known that the models proposed up to now are divided into two categories, mixture (and interstitial) model and continuum model. The mixture model is founded on the flickering cluster model of Frank and Wen,[9] in which liquid water comprises non-hydrogen-

bonded monomers and hydrogen-bonded clusters. The equilibrium between those distinct species changes with the temperature and the pressure. The model assumes that melting of the cluster is accompanied by a shrinkage of volume, analogous to the melting of ice, and thus is able to account for various anomalous properties. This idea was further developed by Nemethy and Scheraga[24] in a more sophisticated model. Many questions arose as to whether hydrogen-bonded clusters could be regarded as distinguishable species.

The origin of the continuum model dates back to Pople.[10] A closely related model called random network model was proposed by Bernal and Fowler.[25] It was assumed in this model that all water molecules take part in hydrogen-bond network. The topological structure of the hydrogen-bond network is retained, although the three-dimensional structure is strained.

The basic ideas of the mixture and continuum models are quite different from each other. Moderate success has been achieved by using each model when appropriate parameters were chosen. Although modeling of liquid water is heuristic in explaining of many anomalous properties of liquid water, each model emphasizes only a certain aspect of this highly associated liquid. Therefore, the underlying assumptions of these models should not be considered to be too realistic. A theory more directly connecting the observed macroscopic properties with the microscopic nature of liquid water has long been awaited.

The situation has dramatically changed since the first molecular dynamics simulation of water by Rahman and Stillinger[14,26] appeared. Most of the properties for liquid water could be reproduced by means of MD simulation with only a simple intermolecular interaction. It was demonstrated that there exists no evidence to support the idea that liquid water is composed of several distinct hydrogen-bonded species and that most of water molecules are connected by hydrogen bonds, although highly strained. Since then, computer simulation[27] has been used to account for the anomalous macroscopic properties of liquid water.[28]

In spite of overwhelming data accumulated by the simulation study, the connection between macroscopic observations and microscopic pictures still remains unresolved. A further development of models of liquid water is one of ways to reconcile the basic concept for both structure and dynamics of liquid water. Another approach is to take full advantage of the simulation results, paying attention to the molecular motions of individual water molecules, in order to examine a putative cooperativity in the dynamic process of liquid water, which is the main subject of this review.

B. Percolation and Random Network Models

A simple, but quite essential, way to investigate hydrogen-bond network connectivity was proposed by Stanley and Teixeira,[12,13] who applied the correlated site percolation[3,29,30] of hydrogen bonds in a lattice model. Although the site percolation model itself was a family of mixture models, liquid water was treated as a large macroscopic space-filling hydrogen-bond network, which is also the fundamental concept imposed on the continuum model. Therefore, further development of this theory could be a promising way to unite two conceptually different ideas of mixture and con-

tinuum models. It is assumed in this model that hydrogen bonds are randomly distributed; there is no correlation among hydrogen-bond formations. A probability for an arbitrary chosen molecule to have i hydrogen bonds, f_i, is given by a binomial distribution

$$f_i = {}_4C_i p^i (1-p)^{4-i} \qquad (1)$$

where p is the probability for an arbitrary chosen pair of the nearest molecules to be hydrogen bonded. Liquid water at room temperature and pressure is well above the percolation threshold ($p_c \approx 0.35$ for ice Ih lattice) for any reasonable hydrogen-bond energy criterion, and three exists a hydrogen-bond network extended over an entire system. Stanley et al.[12,13] showed that, even with this simple assumption, a strong correlation exists among neighboring sites in the hydrogen-bond coordination number. For instance, there exist more four-coordinated water molecules in the neighborhood of the four-coordinated water molecules; the four-coordinated molecules clump together and form clusters. The clusters are called low-density patches, since an ice-like highly hydrogen-bonded region is low in density. Low-coordinated water molecules clump in the same manner. The density fluctuation with various sizes of high- and low-density regions is thus formed.

The hydrogen-bond-forming probability, p, increases with lowering of temperature T. For example, it is assumed to be a linear form of $p = a - bT$,[12] so then the number of four-coordinated water molecules, $f_4 = p^4$ ($i = 4$ in eq 1), increases rapidly when the temperature decreases. The sizes of low-density patches rapidly increase; the density fluctuation thus alters with temperature in highly nonlinear fashion, which they call "amplification mechanism".[12] By relating thermodynamic quantities with this density fluctuation, various anomalies of liquid water were well reproduced. This model also predicts certain dynamical aspects of liquid water. Dynamics of a water molecule is strongly influenced by its coordination number. For example, a water molecule undergoes large rotational motion and causes the dielectric relaxation if more than three of its hydrogen bonds are broken. The probability of such motion taking place is proportional to $f_0 + f_1$ and thus the dielectric relaxation (also many other relaxation processes) of liquid water yields non-Arrhenius temperature dependence.[31]

In spite of the success in explaining many static and some dynamical properties of liquid water, it is not so clear in this model how the actual hydrogen-bond network rearrangement occurs and induces the collective molecular motion and energy fluctuation, which are important in the liquid water dynamics (see below). It was also pointed out that the site percolation model does not include long-range correlation effects of hydrogen-bonds network, which are essential for supercooled water to have a singularity at low temperature.[7,32,33] It is, however, still controversial[34] what kind of phase behavior is involved in supercooled region of water (see section VI.D).

Rice and co-workers[2,11] proposed a random network model to account for thermodynamic and structural properties of liquid water. This approach is an extension of the Pople's bent hydrogen-bond network model.[10] This theory was not based on rigorous statistical mechanics. In this model, the radial distri-

bution function of the oxygen pair was generated by two steps. In the first step, the basic structure was inferred from the analysis of the experimental data, specifically spectroscopic measurements, in a fashion similar to the bent hydrogen-bond network model. In the second step, a further broadening of the radial distribution function by thermal excitation was introduced. The results based on the random network model were extensively compared with those obtained by computer simulation.[2] The model was successful in reproducing properties of liquid water above the freezing point but not below it since a structure reorganization in the low-temperature regime causing a large fluctuation was not taken into account.[7,32-34]

III. Molecular Dynamics Simulation and Intermolecular Potentials

A. Molecular Dynamics Simulation

Technical details for molecular dynamics simulations are well documented in the recent publications.[35] We here describe only a simulation method for an assembly of nonlinear rigid molecules; a large portion of the results presented in this article were obtained by this method. There are various ways to integrate the equations of motion other than this, depending on the potential model used. The reader interested in the methodology of various MD simulations should refer to ref 35. The differential equations to be solved numerically for rigid molecules in the MD simulation here are a coupled Newton–Euler equation of motion:

$$m_0 \frac{d^2 \mathbf{R}}{dt^2} = -\frac{\partial \Phi}{\partial \mathbf{R}} \tag{2}$$

$$\mathbf{I} \cdot \frac{d\omega}{dt} = \mathbf{A} \cdot \sum_\alpha \mathbf{r}_\alpha \times \left(-\frac{\partial \Phi}{\partial \mathbf{r}_\alpha} \right) + \omega \times (\mathbf{I} \cdot \omega) \tag{3}$$

where Φ is the potential function of the system and $\mathbf{R}$ and $\mathbf{r}_\alpha$ are the coordinates of the center of mass and α-th site on each molecule. The mass of water molecule is denoted by m_0 and the inertial moments along principal axes are denoted by $\mathbf{I}$ (consisting of only diagonal elements I_1, I_2, and I_3) and the corresponding angular velocity is ω. The matrix $\mathbf{A}$ stands for the rotational matrix from space to body-fixed coordinates.[36] These equations are solved by Gear's predictor–corrector method; the fifth order for translational motions and the fourth order for rotational motions.[37] A relation between angular velocity, ω, and orientational parameter should be established for the description of a complete set of equation of motion. Quaternions are conveniently used as orientational parameters instead of Euler angles since a singularity at $\sin \theta = 0$ is included in the equation of motions represented by Euler angles.[38] The matrix to describe rotation is expressed by quaterions, and their time dependence is also given by a simple form of angular velocity. To handle the long-range interaction, either Ewald sum[39] or smooth truncation is adopted. The truncation is performed by multiplying by the switching function.[18]

B. Intermolecular Interaction

In molecular dynamics and Monte Carlo simulations, an intermolecular interaction for water molecule is, of course, one of the most crucial factors, upon which reliability of the analysis depends. The potential energy of an assembly of N water molecules, Φ_N, is formally written in the absence of the external field as

$$\Phi_N = \sum_{i<j} \phi_2(\mathbf{r}_i, \mathbf{r}_j) + \sum_{i<j<k} \phi_3(\mathbf{r}_i, \mathbf{r}_j, \mathbf{r}_k) + \cdots \cdots \tag{4}$$

where ϕ_2 is the dimerization energy and ϕ_3 is three-body interaction, which cannot be described by the sum of the dimerization energy. Each potential term depends on both the center-of-mass positions and orientations of molecules abbreviated by $\mathbf{r}$. It is believed that interactions higher than two-body interactions contributes up to 20% of the total energy[40] and therefore it significantly affects the structure and the thermodynamic properties of water. The nonempirical potential, in general, is purely a two-body interaction. Clementi and co-workers[41] obtained higher body interactions and demonstrated that an inclusion of the higher body interactions gives a better agreement of structural properties with experiment. However, the treatment of the higher body interactions is very complicated. On the other hand, the higher body interaction is, although somewhat averaged manner, taken into consideration as an effective potential in empirical potentials. Recently, an induced dipole interaction has also been included in some potential function, introducing a polarizability.[42]

The empirical potential functions called BNS and ST2 models were used in the earlier work by Rahman and Stillinger.[26,43] These potential functions are composed of four point charges. Clementi and co-workers developed a method to construct an intermolecular interaction for water dimer on the basis of *ab initio* molecular orbital (MO) calculations for various mutual configurations. They are known as MCY, CH, and CC potentials,[44] and these give a good account of the structural properties of water. However, they fail to reproduce thermodynamic properties because the higher body interactions are neglected in these functions. A completely different strategy was taken by Berendsen *et al.*;[45] the parameters of the potential funciton are determined so that the pressure and the energy from the simulations agree with experiments. This potential, referred to as SPC potential, has been used in many computer simulations. A similar idea was used by Jorgensen and co-workers to construct a series of TIPS potentials.[46]

Most of the pair potentials comprise point charges, which are located on the atoms and/or other auxiliary sites, in order to mimic hydrogen bonds in small molecular separation and an electrostatic multipole interaction in large separation. The obtained structure is dependent largely on the choice of parameters included in the potential function. One of the most sensitive tests is to check whether a potential can reproduce an appearance of the second peak in oxygen–oxygen pair correlation function, $g_{OO}(r)$. In Figure 1, $g_{OO}(r)$ for the original TIPS (three site model in TIPS family) water and SPC water and $g(r)$ for Lennard-Jones (LJ) fluid are depicted. Although the first peak position is almost the same in those three liquids, the second peak position is quite different in each pair potential. The second peak in an LJ liquid appears at twice the first peak. Unlike simple liquids such as the LJ fluid, the second peak in SPC water locates at 1.6
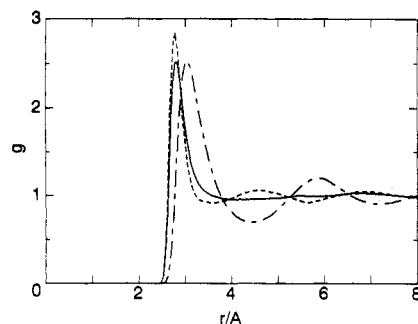
Figure 1. Radial distribution functions for oxygen atoms of liquid water at 298.15 K and for centers of gravity of LJ fluid. The solid line is for TIPS water; the dashed line, for SPC water; the dash–dot line, for LJ fluid.

Figure 2. Schematic representation of the sequential quenching along a trajectory. Instantaneous structures in the trajectory at time $t = t_1, t_2, t_3$, etc. are quenched into the corresponding local energy minima (inherent structures) on the total potential energy surface. One-dimensional picture.

times the distance of the first peak. This peak position indicates that tetrahedral structure remains the same in liquid water as in ice. The second peak was indeed observed experimentally.[47] In both TIPS and SPC potentials, $g_{OH}(r)$ and $g_{HH}(r)$ suggest that a large fraction of molecules are hydrogen bonded. An interesting fact is that while both the original TIPS and SPC potential have the same functional forms, the second peak in $g_{OO}(r)$ is reproduced only in SPC water. Therefore, the location of the second peak is a stringent test of water potential and is very sensitive to the choice of the parameters. A detailed discussion is given by Pangali et al. and by Finney et al. in their review articles.[48] These potential functions were tested for reproduction of not only liquid-state properties but also lattice structures and spectroscopic data in solid state.[49-51]

There is no a priori reason to neglect the intramolecular vibrational motions. Rahman et al.[52] proposed a so-called central force model, in which the intramolecular vibrations are included and all atomic interactions are equivalently treated in both intra- or intermolecular interactions. Use of a central force model[52] is essential when a coupling between intra- and intermolecular motions is important and when a simulation is performed for the chemical reactions in which the atomic exchanges occur. It is, however, difficult to describe both intra and intermolecular interactions by a common functional form. Development of the central force type models remains at a rather primitive stage in comparison with the more successful rigid-rotor model.

The results presented in this review were mostly calculated by employing the TIPS2 potential. The periodic cubic boundary condition for a system with 64 or 216 water molecules was used. The standard MD calculation with the constant volume and the constant energy was used. The average temperature of the trajectories is 298 K.

IV. Inherent Structures of Water

The potential energy hypersurface for a system with many particles consists of an enormous number of potential wells. A minimum-energy configuration in each potential energy well is called an "inherent structure". Stillinger and Weber[15,16] have shown how thermodynamic functions and dynamical behavior of liquids and clusters can be analyzed in terms of the inherent structures. An instantaneous configuration of a system can be separated into two elements, a
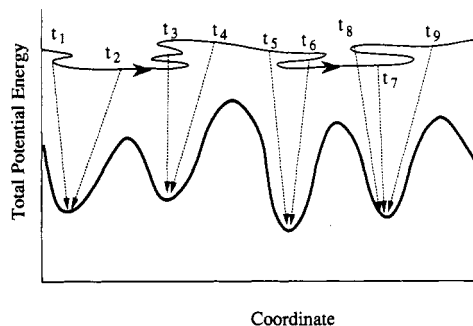
fundamental structure (inherent structure) and a distortional displacement from it. In inherent structures, by removing distortional displacements, the hydrogen-bond network pattern of liquid water is more clearly defined than in instantaneous structures.[17,18,53] In dynamics, the configurational change can be separated into the fundamental structural change (transition of the inherent structures[15-18]) and the vibration in each well. Removing the vibrational components from the dynamics, we can more clearly analyze the fundamental structural rearrangement of the hydrogen-bond network in liquid water dynamics.[16-19,53]

A variety of inherent structures exist in a system with many particles; there are a few very deep minima corresponding to polymorphic crystal structures, and there are deep-energy inherent liquid structures or shallow energy inherent liquid structures. A full set of inherent structures can be calculated only for small clusters;[20] there are only four distinct inherent structures in Ar_7. But, the number of inherent structures increases very rapidly for larger systems; the number is proportional to $\exp(\alpha N)$ where N is the number of particles in a system and α is a constant.[15,20]

A. Inherent Structures along Trajectory

The inherent structures of larger systems were calculated along a trajectory. An instantaneous structure in the trajectory at a time t, $R(t)$, is quenched to the local minimum of the total potential energy, $Q(t)$. The sequential configurations in certain time intervals, $t_n = n\delta t$, are quenched, $R(t_n) \rightarrow Q(t_n)$, as shown in Figure 2. The quenching is performed by using either a steepest descent method, a conjugate gradient method,[54] or a combination of the two.

In the steepest descent method, we solve

$$m\frac{\partial r}{\partial s} = -\frac{\partial \Phi(r)}{\partial r} \tag{5}$$

where the total system configurational vector r with $6N$ dimension for N water molecules, expressed with the Cartesian coordinates of molecular centers of mass and Euler angles of molecular orientations ($\theta_i, \psi_i, \varphi_i, i = 1, 2, ..., N$), starts with an instantaneous configuration $R(t)$ and converges to an inherent structure $Q(t)$, m is a mass tensor, and s is a steepest descent step length. Instead of direct calculation of the derivatives of potential energy Φ with respect to the Euler angles in eq 5, a transformation from torques N is much

advantageous, which is given by the following equations as[55]

$$-\frac{\partial \Phi}{\partial \theta} = N_x \cos \psi - N_y \sin \psi$$

$$-\frac{\partial \Phi}{\partial \varphi} = N_x \sin \theta \sin \psi + N_y \sin \theta \cos \psi + N_2 \cos \theta \qquad (6)$$

$$-\frac{\partial \Phi}{\partial \psi} = N_z$$

where N_x, N_y, and N_z are torque around principal axes of a water molecule.

It should be mentioned that the term "quenching" is not the same as that used in annealing process of amorphous material to its global or semiglobal minimum.[56,57] Here it means a way to find the closest local minimum. The number of steepest descent steps required for the quenching of a configuration is about 20 000–50 000 or even more. It is equivalent to a 8–20-ps trajectory calculation in such as a water system. Almost the same computational time is required in the conjugate gradient method, since the construction of a Hessian matrix (second energy derivative matrix) at each step consumes a lot of computational time, although the number of quenching steps needed is much less. One may also directly evaluate the analytical second-order energy gradients and use them in the Newton–Raphson type procedure. Since it is very time consuming to determine many inherent structures of large systems, the time interval used in sequential quenching along a trajectory must be carefully chosen. If it is too small, many sequential configurations are quenched to the same inheent structure before jumping to the next inherent structure, and so it is computationally inefficient. On the other hand, if it is too large, many inherent structures can be missed. An optimal time interval depends on the temperature and size of the system. For a low-temperature trajectory of a small Ar cluster, it could be from 10 femtoseconds (fs) to a few picoseconds (ps). For a room temperature trajectory of liquid water with 216 water molecules, it is about 2–10 fs or even smaller.[17,18]

Stillinger and Weber performed the inherent structure analyses on atomic and water molecular "clusters".[15,16] They found that the inherent structures are different in different temperature trajectories; the configurations in a high-temperature trajectory are quenched generally to high-energy local minima (inherent structures) of amorphous type, while those in a low-temperature trajectory result generally in the lower energy inherent structures. Comparing the potential energy of instantaneous and corresponding inherent structures before and after the melting of water, they showed how the latent heat of melting ice is distributed to the following elements: 85–90% of the latent heat is attributed to upward shift in potential energy of inherent structures across the transition, and the remainder to changing anharmonicity of potential well curvature.[16]

As the temperature increases, the measure of the system at low-energy inherent structures decreases rapidly because the number of available amorphous type higher energy inherent structures increases and the system moves to the new inherent structures. It is
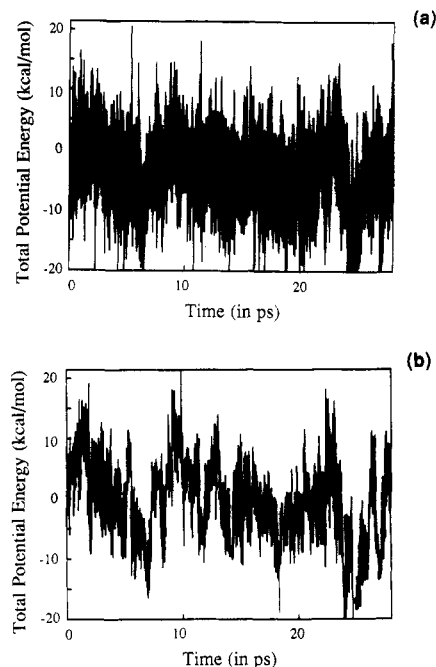

Figure 3. Fluctuation of the total potential energy of the system along the 28-ps trajectory in a system with 64 water molecules: (a) the instantaneous structure energies (real energies along the trajectory) averaged over some time intervals [eq 7 with $\Delta t = 10$ fs]; (b) the corresponding inherent structure energies in 10-fs intervals. Time is in picoseconds and energies in kcal/mol. Energies are relative to arbitrarily chosen standard values as zero. $T = 298$ K.

suggested (see section VI.D) that, as the temperature lowers in supercooled region of liquid water, the homogeneous nucleation from liquid water to an ice structure takes place without being intercepted by the glass transition.[32,33] This phase behavior of the supercooled water is the subject of a current debate.[34] It is important to investigate what kind of global landscape the water potential energy surface must have in order to understand the metastable water properties.

The time sequential quenching procedure furnishes a tool to extract fundamental structure changes in liquid dynamics, by removing its vibrational components. It is meaningful only when the character of instanteous structures is reflected in the corresponding inherent structures. In the liquid Ar case, the quenching, in which the system volume is kept constant, leads to an inherent structure which is quite different from the corresponding instantaneous structure. The inherent structures are in the form of heterogeneous clusters since the volume of liquid Ar shrinks about 10–15% in the phase transition to the solid phase. The situation is different in liquid water; its volume increases in the phase transition to an ice structure. When the volume is kept constant in the quenching procedure, the structures are kept homogeneous; the inherent structures must be a good representation of the corresponding instantaneous structures. This can be checked, for example, by comparing the total potential energy fluctuations of liquid water in the instantaneous structure and in the corresponding inherent structures[17,18] which are plotted in Figure 3, parts a and b, respectively. The instantaneous structure energy averaged over 20 fs ($\Delta t = 10$fs) is plotted in Figure 3a. When a longer averaging time, such as 400 fs ($\Delta t = 200$ fs in eq 7), is used to average instantaneous structures,

$$\tilde{V}(t) = \frac{1}{2\Delta t}\int_{-\Delta t}^{\Delta t} V(t + \tau)\,d\tau \qquad (7)$$

the energy fluctuation corresponds to the energy change in so-called V (vibrationally averaged) structures.[17,58,59] We can see that the overall shape of inherent structure energy fluctuation (Figure 3b) is similar to instantaneous structure fluctuation (Figure 3a), although the magnitude of variation is smaller in the latter; the inherent structures are indeed a good representation of the instantaneous structures. The way the dynamics picks up details of the potential energy surface depends on the kinetic energy (temperature) and the time scale of observation. At low temperature, the molecular motions are strongly constrained by the intermolecular interactions. At high temperature, individual molecular motions are free from the hydrogen-bond constraint, and only the sharp repulsive core part of intermolecular potential is important. On the long time scale, the liquid dynamics is considered to be diffusional and the details of the potential energy surface are averaged out, while the potential energy surface information is more important in short time scale.

An inherent structure is a local potential energy minimum of the total system, not of individual molecules. Liquid water is a "frustrated" system; upon melting from ice, water absorbs the latent heat 1.4 kcal/mol (10–15% of the total binding energy per molecule), and the hydrogen bonds are partially broken. There exist a few very unstable individual molecules in each inherent structure. The wide distribution of the individual water molecular binding energies is seen in Figure 4 in both instantaneous and inherent structures.[17,59] The relative deviation of the individual molecular binding energies $V_i(t)$ in an instantaneous structure, is 0.18 in liquid water (at 298 K).

$$\xi = \sqrt{[V_i(t) - \langle V_i\rangle]^2/\langle V_i\rangle^2}. \qquad (8)$$

ξ is 0.11 in liquid Ar (at 95 K). Here the average $\langle V_i \rangle$ is over all molecules (atoms) and the ratio ξ is averaged over many instantaneous structures. Besides, the amplitude of the average binding energy is large for the liquid water, $\langle V_i \rangle = -20$ kcal/mol. An energy difference between the most stable water molecule and the most unstable one reaches up to 20 kcal/mol. Stability or instability of individual molecules changes with time. In Figure 5, we can see that, on average, a water molecule becomes very unstable once every 10 ps. This fast and large energy fluctuation in liquid water is different from other liquid or cluster dynamics.

The total potential energy fluctuation is also large in liquid water as seen in Figure 3. But the deviation ratio of the total potential energy $V(t)$ in time t is about 0.01 for liquid water, which is about the same magnitude as in other liquids, for example, $\zeta = 0.01$ for liquid Ar.

$$\zeta = \sqrt{[V(t) - \langle V\rangle]^2/\langle V\rangle^2} \qquad (9)$$

Here, $\langle V \rangle$ is the time average of the total potential energy, $V(t)$. This shows the large energy fluctuation in liquid water is attributed only to a large hydrogen bond energy [the large amplitude of $V(t)$]. The large individual molecular energy fluctuations are mutually canceled partially in the total energy:
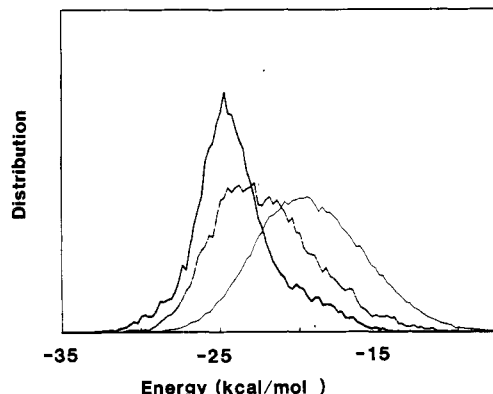

Figure 4. Distributions of individual molecular potential energy V_i in the instantaneous structure (—); in the V structure (eq 7 with Δt = 200 fs) (− −); and in the inherent structure (——). Distributions are normalized; the system has 216 water molecules in TIPS2 potential; T = 298 K; energies are in kcal/mol. (From ref 17.)
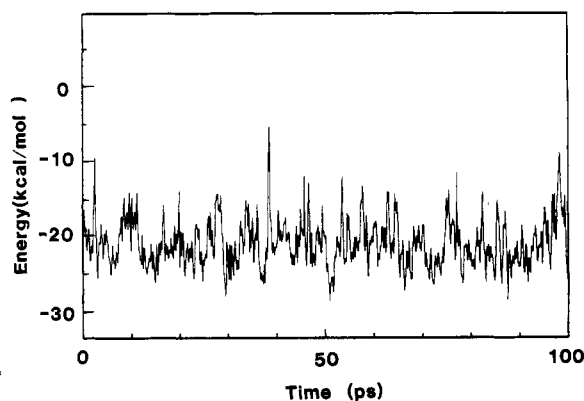

Figure 5. Potential energy of individual water molecule along the trajectory. A water molecule is arbitrarily chosen. Potential energy, V_i, in the V structure (the water binding structure averaged over fast vibrational modes (eq 7 with $\Delta \tau$ = 200 fs) is plotted. Figure shows the 100-ps trajectory for a system with 216 water molecules; T = 298 K; energy is in kcal/mol; time is in picoseconds (10^{-12} s). (From ref 17.)

$$V(t) = \frac{1}{2}\sum_{i=1}^{n} V_i(t) \qquad (10)$$

Flip–flop type energy exchanges exist among neighboring water molecules.[17] It should be mentioned here that the frequency component of the total potential energy fluctuation $V(t)$ in liquid water is quite different from many other liquid cases, although their values of the ratio ζ (eq 9) are similar. Liquid Ar potential energy fluctuates as a white noise, while liquid water yields so called $1/f$ noise behavior (see section VI).

B. Collective Motions

In liquid (cluster) dynamics, the particle motions are strongly correlated and induce collective motions. One can quantify how motions are collective in liquid (cluster) by calculating the moment ratio:

$$\gamma(t_n) = \frac{\langle \Delta\mathbf{r}(t_n)^4\rangle}{\langle \Delta\mathbf{r}(t_n)^2\rangle\langle \Delta\mathbf{r}(t_n)^2\rangle} \qquad (11)$$

where $\Delta\mathbf{r}(t_n)$ expresses the displacement of a molecule in a transition from an inherent structure, $\mathbf{Q}(t_n)$, to the successive inherent structure, $\mathbf{Q}(t_{n+1})$ ($\Delta t = t_{n+1} - t_n$ is

the interval used for the sequential quenching of the trajectory), and ⟨ ⟩ means the average over all molecules in the system. Stillinger and Weber[15,16] applied this moment ratio in the analysis of the atomic/molecular cluster dynamics. The value of this quantity γ is $5/3$, if the distribution of the particle displacement $\Delta \mathbf{r}$ is Gaussian, and so $3/5\gamma - 1$ is called the "non-Gaussian parameter" and used to quantify collective molecular motions in the glass state. If the molecular displacements are widely spread (delocalized) in space, γ is close to unity, while if they are completely localized, γ is in the order of the total particle number N.

Ohmine *et al.*[17] used this moment ratio, γ, to analyze liquid water dynamics and found that the molecular motions in liquid water are quite collective. They calculated the moment ratio for molecular displacement

$$\Delta \mathbf{r}^2 = \sum_{i=1}^{3}(\Delta x_i^2 + \Delta y_i^2 + \Delta z_i^2) \qquad (12)$$

where Δx_i is Cartesian coordinate displacement of the i-th atom (i indicates O or H) in a water molecule. The value γ, averaged over 400 inherent structure transitions in which at least one of water molecules moves more than 1 Å $[(\Delta \mathbf{r}^2)^{1/2} \geq 1$ Å$]$ in a system with 216 water molecules (with $T = 297$ K and the quenching time intervals $\Delta t = 10$ fs), is about 11. It means that about 20 water molecules move simultaneously. The moment ratio can be calculated in terms of the center-of-mass motion γ_{cm} and of the Euler angle γ_{ang} (six variables), instead of Cartesian coordinate of the O and H atoms (nine variables). The values of the moment ratio in the former expression ($\gamma_{cm} = 11$ and $\gamma_{ang} = 12$) are very similar to that in Cartesian expression ($\gamma = 11$).

We can visualize the degree of similarity among fundamental structures (inherent structures) by analyzing the distance between two inherent structures at time t_n and t_n' (the distance matrix)

$$R(t_n, t_n')^2 = |\mathbf{Q}(t_n) - \mathbf{Q}(t_n')|^2 \qquad (13)$$

where $\mathbf{Q}(t_n)$ and $\mathbf{Q}(t_n')$ are the inherent structures corresponding to the system configurations in the trajectory at time t_n and t_n', respectively. The darker shade is marked on Figure 6 if the distance between $\mathbf{Q}(t_n)$ and $\mathbf{Q}(t_n')$ is closer; Figure 6 is the distance matrix for a system with 64 water molecules (see also Figure 5 in ref 18). If molecular motions are diffusive and there are no collective displacements, this matrix forms a band structure. If they are intermittent, it forms island structures.[18]

We can see in the figure that the global structure of the distance matrix consists of several islands. The inherent structures belonging to the same island are similar in geometry. The island-to-island transitions, called "overall inherent structure transitions", involve large collective motions. A typical example of collective motion in a 216 water molecule system is shown in Figure 7.[17] We can see that a collective motion consists of a few tens of molecular displacements localized in space. A collective motion occurs once in sub-picoseconds, while small inherent structure transitions occur once every 13 fs for the system with 64 water molecules (at 298 K);[18] tens of small transitions occur between collective transitions. We can further see within each island in Figure 6 that there exist fine structures in the
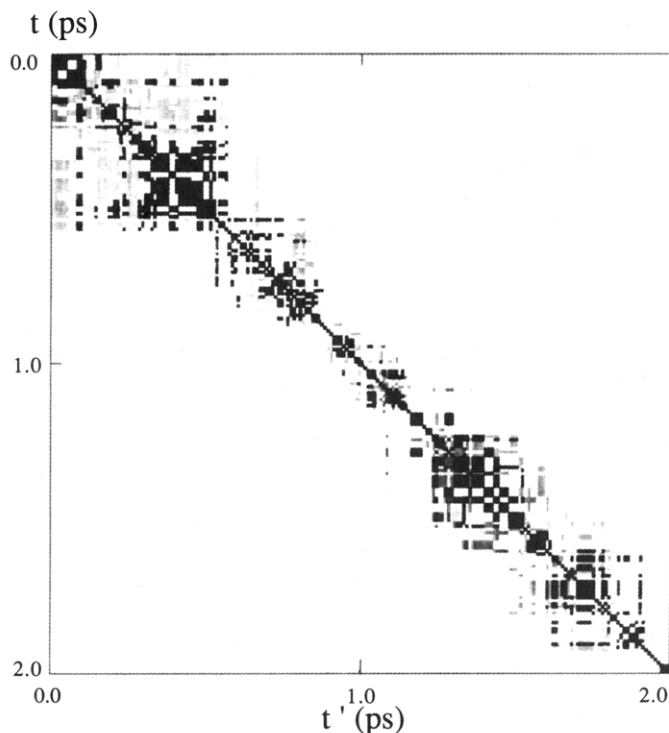

Figure 6. The distance matrix (eq 13) for inherent structures. The matrix $R(t_n, t_n')$ is marked with a shade square in the figure if the distance between the inherent structures $\mathbf{Q}(t)$ and $\mathbf{Q}(t')$ is $R(t,t')^2 < 160$ Å^2. Each square is shaded with a different degree of darkness accordingly to the value of $R(t,t')^2$. The shade is darker when the distance is shorter. There are 7 degrees of darkness. The inherent structures successively visited by the system in a trajectory for a system with 64 water molecules; $T = 298$ K; 200 inherent structures in 10-fs intervals are used (1 fs = 10^{-15} s); TIPS2 potential was used.
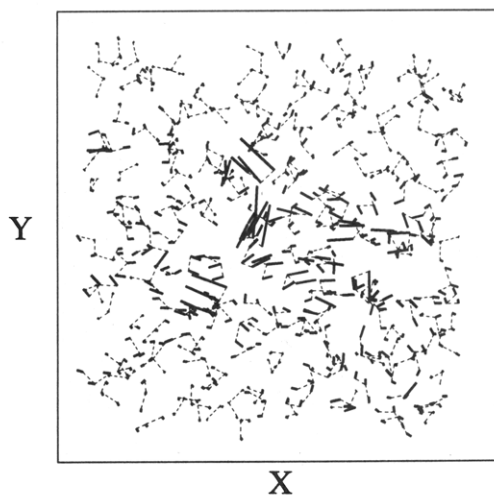
Figure 7. Collective motions in liquid water. For a system with 216 water molecules, the figure depicts water molecular displacements in a transition from an inherent structure to the next inherent structure in a trajectory. The heavy solid lines indicate the displacements of individual atoms of water molecules. The O–H bonds of the individual water molecules before the transition are indicated by the dotted lines. $T = 298$ K. TIPS2 potential was used.

shaded pattern. This means that liquid water dynamics undergoes many small but a kind of hierarchical molecular movements within a large basin (within each island), then makes a large jump to the next large basin (island–island transition), and so the motion continues.

The mapping of the distance matrix is meaningful only for small systems or for subsystems in a large system. In a large system, collective motions occur independently in space (in each subsystem). The distinct island structures in each subsystem disappear because of their overlaps. The distance matrix thus becomes a near-band matrix in a large system. It was also found that there is a minimum system size to yield such collective motions (and fluctuations); a system must contain at least about 30 water molecules.[17]

It should be mentioned that eq 13 is a *scalar* quantity representing the structural similarity. There are many other ways to represent molecular motions. In order to analyze the hydrogen-bond network reordering mechanism in more detail, some *vector* quantity, quantifying the topological index of the hydrogen-bond network, must be invented. A simple method of this type is to compare the hydrogen-bond patterns[60] which alter along the trajectory.

Sciortino et al.[53] also used the inherent structures to investigate the effect of defects on molecular mobility in liquid water. The quenching removes vibrational elements from the dynamics and thus the hydrogen bonds[61] can be well defined in inherent structures. They analyzed the molecular mobility in the low-temperature and low-density water dynamics, where the defects can be defined relative to the tetrahedral hydrogen-bond structures. They indicated that the five-coordinated water molecules attached to this tetrahedral structures are the topological defects and act as a catalyst to induce a transition between different tetrahedral local arrangements in low-temperature dynamics;[53] these defects provide low-energy paths of such rearrangements by the flip–flop energy exchange mechanism. It is found, however, that three- and four-coordinated water molecules, as well as five-coordinated molecules, are involved in the hydrogen-bond rearrangement dynamics in the room temperature trajectory.

C. Neutron Scattering

The inelastic neutron scattering (INS) technique is a very useful tool to observe collective motions in liquids.[62] In this technique one can simultaneously measure the displacement and momentum transfer of particle motions. Due to the recent development of this technique, it is now possible to observe experimentally the collective motions in liquid water, just discussed above. Teixeira et al.[63–66] performed the incoherent quasielastic and coherent inelastic neutron scattering studies on light water and heavy water. They analyzed two components related to the hydrogen-bond network rearrangement dynamics: (1) one component contributing to the line width of the scattering peak appeared in incoherent quasielastic neutron scattering of H_2O;[63] and (2) the second component appeared at the shoulders of central scattering peak in the coherent inelastic neutron scattering of D_2O.[64] Neutron scattering experimental data and their analyses were reviewed by Chen[65] and by Bellissent-Funel et al.[66]

The first component (1) was attributed to diffusional motion of an individual water molecule. It was further decomposed into a hindered rotational element (with relaxation time τ_1) and a translational jumping diffusional element (with residence time τ_0). Teixeira et al.[63] found that the residence time τ_0 of the translational

jumping diffusion yields non-Arrhenius temperature dependence, while the hindered rotational relaxation time τ_1, which is considered to be the lifetime of a hydrogen bond, is Arrhenius with an activation energy 1.85 kcal/mol. It was assumed that the translational diffusion is influenced by the hydrogen-bond network rearrangement, and it can take place only when more than three hydrogen bonds of a molecule are broken. If the correlated site percolation model of Stanley et al.[12,13] is used, the probability of such a jump taking place is proportional to $f_0 + f_1$, where f_i are given in eq 1, which is non-Arrhenius.[65] A similar argument is used by Salvetti et al. to explain the non-Arrhenius temperature dependence of the dielectric relaxation time τ_r ($1/\tau_r$ is proportional to $f_0 + f_1 + f_2$) for supercooled water.[31]

The second component (2) is the collective excitation propagating at 3310 ms^{-1}.[64,66,67] This speed is more than twice that of the normal sound velocity. The high-frequency sound was interpreted as some kind of collective molecular motions of localized regions which extend to about 10-20 Å in length. It was attributed to the motion of the hydrogen-bond patches, defined in section II. There is no detailed study on the temperature dependence of this component. Deriu et al.[68] also found similar collective water molecular movements in the quasielastic neutron scattering of dilute aqueous gels.

It is very important to analyze the dynamical structure factor of the neutron scattering, $S(\mathbf{q},\omega)$, in terms of the inherent structures, in which the motional components can be clearly separated into the fundamental structure rearrangement element and the vibrational element. Components 1 and 2 may be attributed to the motions appearing in the distance matrix of Figure 6. Small inherent structure transition occurring within an island[18,19] in Figure 6 may correspond to the jump diffusion in configuration space 1. Large intermittent movement (an overall inherent structure jumping)[18] in Figure 6 corresponds to the collective motion found in coherent inelastic neutron scattering 2. It is noted that the rotational motion and translational motion are strongly coupled in liquid water dynamics as we will see in section VI.A. Thus the functional form,[63,65] used to decompose the component 1 into the rotational and translational diffusional elements, should be improved.

D. Reaction Coordinates and Energy Barrier Heights

In order to understand the nature of the inherent structure transition, the reaction coordinates (RC) connecting inherent structures and their transition states (TS) are to be determined.[69] There are a few methods to find RC and TS for systems like liquids with very many degrees of freedom. Two types of methods are used to determine RC and TS. The first group is known as the climbing hill methods; among these the best-known methods are the method proposed by Cerjan and Miller[70] and the gradient extremal method developed by Ruedenberg and co-workers.[71] They are stepwise climbing hill methods on a potential energy surface with a certain initial condition. Different initial step directions lead to different RCs and TSs. The initial step direction from the minimum (inherent

structure) is chosen to be one of its normal mode vectors. A subsequent climbing step direction is chosen to be a normal mode vector at each grid point on RC, which is close to the previous step vector. The gradient extremal method further imposes a condition that the gradient to the equipotential-energy contour must be extremal at each grid point on RC and yields a marked convergence, while the Cerjan–Miller method without such a condition sometimes has a convergency problem. The second group of methods searches RC by starting from approximate paths or transition states (TS); Elber and Karplus[72] first proposed a practical method to obtain approximate RC for systems with very many degrees of freedom by minimizing the average value of the total potential energy along a path:

$$S = \frac{1}{M\Delta l}\sum_{j=1}^{M}E(\mathbf{r}_j)\Delta l_j + \lambda\sum_{j=1}^{M}(|\Delta\mathbf{l}_j| - \Delta l)^2 \quad (14)$$

where

$$\Delta l = \left(\sum_{j=1}^{M}\frac{(\Delta l_j)^2}{M}\right)^{1/2}$$

with respect to $M - 1$ grids points $\mathbf{r}_j$ ($j = 1, ..., M - 1$). Here $\mathbf{r}_j$ is an n-dimensional position vector (e.g. $n = 1296$, for a system with 216 water molecules) representing the water structures of the total system at the j-th grid point on RC ($\mathbf{r}_0$ and $\mathbf{r}_M$ are two inherent structures which are connected by RC), $E(\mathbf{r}_j)$ is the potential energy at a grid point $\mathbf{r}_j$, and $\Delta\mathbf{l}_j$ is the line vector pointing from the grid point $\mathbf{r}_{j-1}$ to $\mathbf{r}_j$, and Δl_j is its length. The second term in right-hand side of eq 14 imposes the condition that all line segment Δl_j are equidistance equal to Δl, and λ is the Lagrange multiplier. To locate the exact TS from approximate TS obtained by this Elber and Karplus method, one can use the McIver and Komornicki method[73] minimizing the norm of the potential energy gradient. Reaction coordinates are then determined as the steepest descent paths from the exact TS.[74]

Elber et al. proposed another iterative method searching for RC by steepest descent method.[75] In their method, the initial grid points are located on an approximate path. A grid point in the next iteration is chosen to move from a present grid point ($\mathbf{r}_j$) to the direction (ρ_j) of the orthogonal to the line segment between this grid point ($\mathbf{r}_j$) and the next lower energy grid point ($\mathbf{r}_{j'} = \mathbf{r}_{j+1}$ or $\mathbf{r}_{j-1}$, whichever is the lower in energy) on RC with the magnitude of the energy gradient along this orthogonal direction:

$$\partial E(\mathbf{r}_j)/\partial\rho_j$$

where $\rho_j \perp (\mathbf{r}_j - \mathbf{r}_{j'})$. The calculation is repeated until all energy gradients along the orthogonal directions become very small. The convervency of this method is slow but may be improved by adapting the conjugate gradient method or by using the analytical second energy gradients. If the number of grids points on RC is infinite, this method leads to the exact RC and TS. Usually, 10–20 grids points ($n = 1, 2, ..., 10$ or 20) are used and thus an approximate TS is obtained.

There are advantages and disadvantages to use each type of methods, as discussed by Elber et al.[72,75,76] and by Case et al.[77] Climbing hill methods can easily find RCs with small energy barriers (TS) and were used in

the analysis for cluster dynamics by Wales et al.[78,79] Convergency of the gradient extremal method has been demonstrated by Shida et al.[80] for two-dimensional case and also applied to Ar clusters. It is, however, hard to choose the correct initial condition which leads to the RC connecting a given pair of neighboring inherent structures. Liquids dynamics often passes through relatively high energy barriers, which are sometimes hard to reach with these climbing hill methods, especially for systems with many degrees of freedom. The second kind of method usually starts from a least motion (LM) path straight connecting two minima[19,64] but, if the initial path is not carefully chosen and far from the seeking RC, often ends up with a wrong RC or a path going through an extra minimum.

Tanaka and Ohmine[18] applied Elber and Karplus's method to obtain approximate RCs, connecting the successive inherent structures visited by the water system in the trajectory. The barrier height averaged over 60 RCs was found to be about 3 kcal/mol in the liquid water system with 64 water molecules. More important is the finding that the barrier energies of the transitions between "overall inherent structures" are in general small, within a few kilocalories per mole. A low-energy pathway connecting one potential energy basin to the next (involving large hydrogen-network rearrangement but with a small energy barrier) is narrow in phase space. With sequential small inherent structure transitions, the system is gradually adjusted to make such a large transition. This dynamics is similar to the jump diffusion described by the free-volume theory[81] for the hard-sphere model. In liquid water there are indeed many free-volume spaces (cavity), which have a sharp size distribution (see section VIII).[82,83] But water molecules around those simple cavities are not necessarily involved in large displacements.

Barrier energy heights along RCs are usually $1/3-1/5$ of those along the least motion paths (LMs);[18] individual molecular motions are strongly correlated. As we will see below, a reaction coordinate overlaps mainly with very low frequency normal modes, which mostly consist of translational components, and with the intermediate frequency modes, which consists of very localized hindered mainly translational and some rotational components, where those normal modes are calculated at the initial or final inherent structure of the reaction coordinate.[18]

Wales et al.[21,78,79] applied the Cerjan–Miller method to Ar and other molecular clusters. The isomerization dynamics among various conformations of clusters and its temperature dependence were analyzed in terms of inherent structures and reaction coordinates. They related the "melting transition" of small clusters to their barrier height distribution. Recently, Wales et al. extended their calculation to water clusters.[84]

As seen in section IV.A, individual molecular potential energies exhibit very large energy fluctuations, sometimes reaching up to 20 kcal/mol (Figure 5). The total system potential energy yields relatively small energy fluctuations in comparison with these individual molecular fluctuations, although the total energy fluctuation in liquid water is larger than those in other liquid systems. This is because there are seesaw-type energy exchanges[17] among individual molecules (i.e., as a
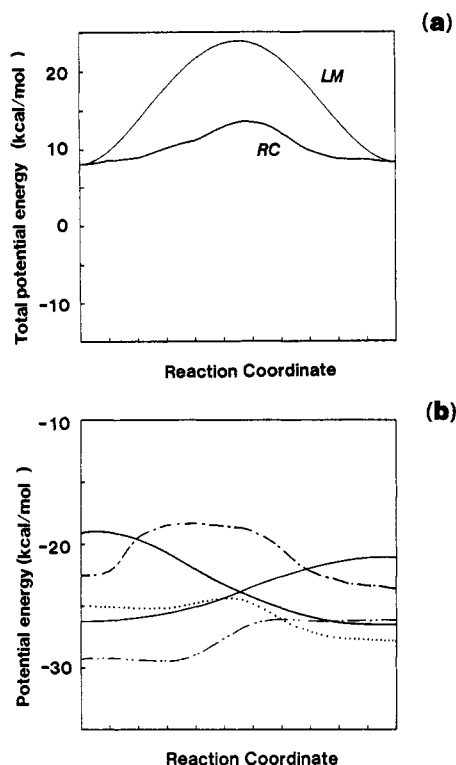
Figure 8. Total potential energy of the system (a) and the potential energy of individual water molecules (b) along a reaction coordinate. In a the reaction coordinate energy (RC) and the least motion path energy (LM) are plotted. In b 5 out of total 64 water molecules in the system are selected, for the system with 64 water molecules in TIP4P potential. Total energy is relative to a standard energy as zero and the potential energies of individual molecules are in absolute energy. Energies are in kcal/mol. $T = 298$ K. (From ref 18.)

molecule is stabilized, another is destabilized).[18,53] With this seesaw-type energy exchange mechanism (see eqs 8–10), the system causes large individual energy fluctuations with a small total energy change and small kinetic energy. (The kinetic energy is proportional to the square of the seesaw motion velocity.) We can see,[19] for example, in Figure 8b that a few individual molecules yield 5-10 kcal/mol potential energy changes, while the total energy yields small change, 3 kcal/mol along a RC (Figure 8a). This shows that water motions are mutually coupled; the hydrogen-bond annihilation and creation are not random process but are strongly correlated. For every 10 ps, an individual water molecule becomes very unstable (individual molecular energy $V_i > -12$ kcal/mol, i.e. two of its four hydrogen bonds are broken), and then usually undergoes large rotational motion to find a new stable bonding structure.[17]

V. Multidimensional Properties of Potential Energy Surfaces

In the previous section, we studied the inherent structures and their transitions along the trajectory. In this section, the multidimensional nature of the potential energy surface of liquid water will be explored.

A. Normal-Mode Analysis

Normal-mode (NM) density of the liquid can be calculated in two ways: (1) by performing a spectral
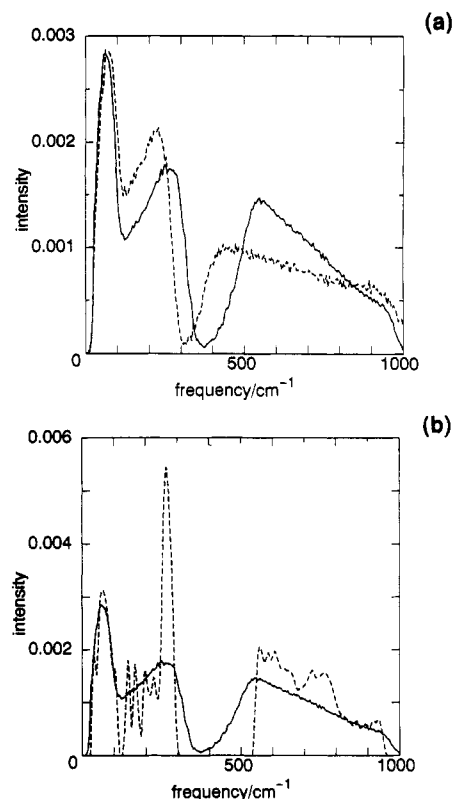

Figure 9. Normal mode distributions of liquid water and cubic ice Ic. In a, solid line is for TIP4P water and the dotted line is for MCY water, each of which is averaged over 40 inherent structures. In b, solid line is for liquid water and the dotted line is for cubic ice. The distributions are over 40 inherent structures of liquid water and 4 structures of proton-disordered ice Ic, for the systems with 216 water molecules in TIP4P potential. Frequency is in cm^{-1}.

resolution of classical mechanical trajectories (Fourier transformation of a velocity autocorrelation function); The method was discussed by Geldard et al.[85] and Martin;[86] and (2) by calculating and diagonalizing a matrix of second energy derivatives with respect to the mass-weighted coordinates.[87,88] The expression of these derivatives with respect to the Euler angles is very complicated. The mass matrix for Euler angles was given by Pohorille et al.[87] The density of state of liquid water was calculated by Rahman and Stillinger using the first method.[14] The precise determination of normal modes by using the inherent structures (the second method) was first carried out by Pohorille et al. for the MCY water potential.[87] They used the normal modes to evaluate a free energy of liquid water. Tanaka et al. determined the normal modes for TIP4P potential.[17,18] The calculated normal-mode density was found to be similar for both MCY and TIP4P potentials,[17,87] except that the peak positions for $\omega > 200$ cm^{-1} are shifted to lower frequencies and the librational modes are more widely distributed in MCY potential as seen in Figure 9a. The normal modes of liquid water mainly consist of high-frequency (450–1000 cm^{-1} in TIP4P potential) librational modes and low-frequency (10–300 cm^{-1}) hindered translational modes.[18,19,87] There are two peaks in the low-frequency band and they are located around 50 and 250 cm^{-1}, respectively. There are some intermediate-frequency (300-450 cm^{-1}) modes, in which localized motions of only few molecules are involved. Their motions are a mixture of mostly translations and some rotations and are associated with the existence of

defects in hydrogen-bond structure in liquid water. These modes are absent in the ice as seen in Figure 9b, in which the mode distributiosn in TIP4P potential is plotted for liquid water and the cubic ice Ic. It is noted that we did not include the intramolecular vibrations, which has the spectral density above 1400 cm^{-1}, in the calculation.

There are two kinds of anharmonicity corrections on a harmonic approximation of a potential well: one with a simple curvature changes from a quadratic form C_2q^2 for a large amplitude motion along a normal vector direction, and the other with mode–mode mixing. The mode-mixing term will be discussed in section V.C. The magnitudes of the former contributions[18] are different in different normal modes; in general the low-frequency modes have a significant positive quartic contribution, C_4q^4 $(C_4 > 0)$, and the high-frequency modes have a large cubic contribution, C_3q^3, where the total mode energy is given by $E(q) = C_2q^2 + C_3q^3 + C_4q^4$ and q is a scalar normal coordinate.

One can make use of normal modes at inherent structures to calcualte the free energy.[21,23] Assuming that each potential well is harmonic, the normal modes and their distribution are determined for a certain set of inherent structures. Pohorille et al.[87] calculated the free energy for harmonic glasses (inherent structures) of liquid water in the MCY potential parameter. The entropy value obtained by this calculation is about 50% of the experimental value for liquid water at 300 K. To calculate the configurational entropy of liquid states correctly, all inherent structures are generated and summed into the partition function. This is, however, impossible for a large system like liquid water. Successful calculations of the free energies are only for small clusters. Wales et al.[21b,84] calculated high-temperature and long-time trajectories and then performed many systematic quenches (thousands of quenches) to obtain the partition functions. The results reproduce the solid–liquid "phase transitions" and S-bent curves, which are in agreement with the simulation results. McGinty[89] suggested that thermal quantities of simple atomic clusters are well reproduced by the harmonic of the potential wells since there is cancellation among higher order contributions. In liquid water calculations, there can be many sources of the errors in the free-energy calculation, such as the error in the intermolecular interaction parameters, and that due to not accounting for anharmonicity effects. A system in the liquid state stays mostly in regions of higher energy potential wells, where anharmonic contributions are often important.

B. Raman Spectrum

In the low-frequency region (ω < 350 cm^{-1}) of the Raman spectrum of liquid water, there exist two distinct peaks one around 50 cm^{-1} (S mode; shear transverse acoustic wave termed by Walrafen et al.[90,91]) and another at 190 cm^{-1} (P wave band according to Walrafen et al.). These peaks have been a central focus of many investigations.[90–93] The calculated normal mode distribution in Figure 9 is very similar to the Raman band shape, except that the latter decays a little faster than the normal mode distribution in the higher frequency region (200–350 cm^{-1}). Characteristics of these bands are (1) there is an isotope effect on S band frequency

while there is no effect on P band and (2) S band yields a slight upward frequency shift as the temperature increases, while the P band shows significant downward shift. The assignment of these two bands were made as follows: the S band is assigned to the O–H...O bending and P is to the O–O stretching of O–H...O unit.

The calculation of the normal modes showed, however, the low-frequency modes are mostly a hindered translational vibration and do not contain bending (librational) element. Mazzacurati et al.[94] and Madden et al.[95] performed the MD calculations for Raman intensity with using polarizability expansion and ascribed the main contribution of the low frequency spectrum to a dipole-induced-dipole element caused by the hindered translational vibrations.

In addition to these two bands, the third vibrational component is claimed to appear at 70 cm^{-1} by Walrafen et al.,[90] as temperature increases. This band is assigned to the bending motion of the bifurcated hydrogen bonds, which arise from the breaking of the firm hydrogen bonds upon the temperature increase. Below these normal mode peaks, there exist Raman intensity components related to the inherent structural transitions (i.e., hydrogen-bond rearrangement dynamics), which will be discussed in section VI.

C. Normal-Mode Excitation and Relaxation

One can explore multidimensional properties of potential energy surfaces of liquid by the following normal-mode excitation. Taking several inherent structures as the initial geometries, the trajectory calculations were performed by vibrationally exciting individual modes with different kinetic energies.[19] Simultaneous excitations of two or more modes can also be performed. How the excited modes relax through mode mixing and how the system undergoes inherent structure transitions after these mode excitations[19] were analyzed. It was then found that most (>95%) of the water normal modes are "inactive", unless they are excited with extremely large initial energies. An inidividual mode in this group couples with only one or two modes of nearby frequency, and thus yields a multiply periodic motion. Only two types of modes, the localized modes and the lowest frequency modes, are active; their excitations yield very fast vibrational energy relaxation and often cause inherent structure transitions. An excited localized mode couples with many double frequency modes through a 1:2 Fermi resonance. It can induce an inherent structure transition when the initial excitation energy exceeds a certain threshold value. Excitations of the lowest frequency modes induce mostly inherent structure transitions. Some of these inherent structure transitions are the same as those induced by the localized mode excitations at intermediate frequency. Indeed, the reaction coordinates of these inherent structure transitions consist of vector elements of the lowest frequency modes and the localized modes.[19]

Excitations of the same mode with different initial energies often result in different inherent structure transitions; bifurcation of the transitions occurs.[19] With small energy excitations of the lowest frequency modes, the transition involving very localized molecular displacements take place. This means that there exist many small "cavities" in liquid water where water
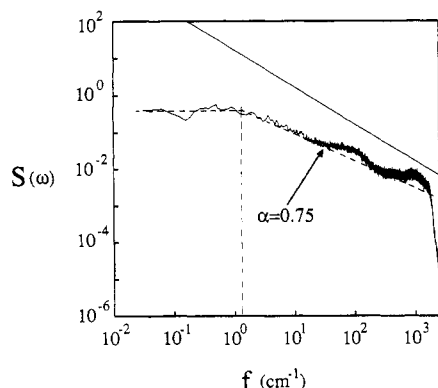
Figure 10. The power spectrum of total system potential energy in the instantaneous structures of liquid water. The system has 64 water molecules at 298 K. f is in wave number (cm^{-1}), and $f = \omega/2\pi$. A trajectory of 5.4 ns is divided into 6 parts, which are Fourier transformed and averaged. Weak Gaussian averaging is used to smooth the spectral curve. A solid line indicates $1/f^\alpha$ with $\alpha = 1.0$, and dashed lines with $\alpha = 0$ and 0.75. The modified TIPS2 potential is used. (From ref 96.)

molecules can easily go through. They are, however, not simple cavities. A moving molecule alters its binding partners, and thus this localized transition involves relatively significant individual pair binding energy changes without a large total binding energy change. When the low-frequency modes are excited with slightly larger energies, collective transitions involving many water molecules are induced. Due to the existence of such bifurcation, liquid water exhibits a variety of motions. In order to understand the higher order mode mixing in the high-energy region of the potential energy surfaces, which must be intrinsic in liquid dynamics, further investigations are required.

VI. Long-Time Behavior of Fluctuation

The average lifetime of individual hydrogen bonds is a few picoseconds at room temperature. But global hydrogen-bond network structures are seen to persist for longer time; liquid water involves many relaxation processes, with many time scales.[96]

A. Power Spectrum of Potential Energy Fluctuation

In section IV.A, we found that the liquid water dynamics involves large potential energy fluctuations such as shown in Figure 3, parts a and b. Here, we examine the power spectrum of the total potential energy fluctuation of liquid water:

$$S(\omega) = |\int_{t_{\min}}^{t_{\max}} V(t)e^{i\omega t}\, dt|^2 \qquad (15)$$

where $V(t)$ is the total potential energy of the system at time t (in a 2-fs interval), Figure 10 shows that there are two regimes in the spectrum at 298 K.[96] In a frequency range (1–100 cm^{-1}) the spectrum yields a $1/f^\alpha$ ($f = \omega/2\pi$, $\alpha = 0.75$) dependence[97] with small peaks corresponding to the normal-mode vibrations of translational and librational motions. Below a low crossover frequency f_c, around 1 cm^{-1}, the spectrum is of a white noise type., There is no memory effect for longer than 30 ps. This 30 ps might be considered as a persistent time of a global hydrogen-network structure in liquid

water dynamics.[96] It is about one order longer than the average lifetime of the individual hydrogen bonds, which is known to be about 2–3 ps. The total potential energy fluctuation, which is equal to the negative of the total kinetic energy fluctuation in a microcanonical MD simulation, represents the temperature fluctuations of the total system. It has been generally recognized that liquid water exhibits a long-time temperature fluctuation in MD calculations and very many steps are needed to achieve a convergency in Monte Carlo (MC) simulations. This type of long-time fluctuation can be attributed to the global hydrogen-bond rearrangement dynamics.

The $1/f$ type frequency spectrum for $f > f_c$ indicates that the correlation of network fluctuations decays not in a single Markovian process but through multiple processes. The number of molecules involved in the network rearrangement motion at each instant is widely distributed. This wide distribution should correspond to the multiplicity of the relaxation processes; a large-scale rearrangement involving many molecules is relatively infrequent and is associated with a long-time relaxation process. A small-scale rearrangement, on the other hand, occurs more frequently and is associated with a shorttime relaxation process. Another possible explanation for this $1/f$ behavior is that the water dynamics can be regarded as intermittent; the system is mostly trapped in a torus (such as a large basin consisting of several inherent structures), and occasionally jumps to another torus. Such intermittent dynamics is known to yield $1/f^2$ ($\alpha = 2$) spectrum when the jump time is close to zero.[98] In real dynamics the jumping occurs in finite duration and is often diffusional, and thus the smaller exponent ($\alpha < 2$) is expected.

The instantaneous structures in the same trajectory as above are sequentially quenched to their inherent structures (see Figure 3, parts a and b).[96] The fluctuation of these inherent structure energies yields a $1/f^\alpha$ power spectrum with $\alpha = 1.3$, a stronger $1/f$ dependence than the instantaneous structure spectrum. The liquid dynamics in the instantaneous structure includes a diffusion from a potential well to the next well and short-time vibrational relaxations, and so the spectrum of its potential energy fluctuation is shifted from the inherent structure's to yield more white and Debye type frequency dependences.

On the other hand, the spectrum of the total potential energy fluctuation for the liquid Ar is almost frequency independent (see Figure 11); that is, liquid Ar dynamics is stochastic and mostly simply diffusional.[96] It is noted here that collective hydrogen-bond network rearrangement in liquid water dynamics consists of both rotational motion and translational motion of the molecules. So when either of these motions is suppressed in an MD calculation, the large rearrangement dynamics (collective motion and energy fluctuation) is also suppressed and the energy fluctuation in the absence of the large inherent structure transition becomes a near white noise (see Figure 12, parts a and b).[99]

B. Very Low Frequency Raman Spectrum

This power spectrum of the total potential energy fluctuation (Figure 11) is similar to the low-frequency component of the Raman spectrum. Figure 13 show the low-frequency part ($\omega = 0.6$–1000 cm^{-1}) of the
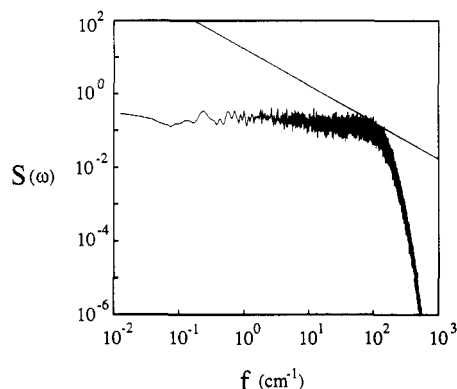
Figure 11. The power spectrum of the total system potential energy in liquid Ar (the system with 108 Ar atoms at 95 K). A trajectory of 6 ns is divided into 2 parts, which are Fourier transformed and averaged. Weak Gaussian averaging is used. A simple Lennard-Jones potential is used. f is in wave number (cm^{-1}). A solid line indicates $\alpha = 1.0$. (From ref 96.)
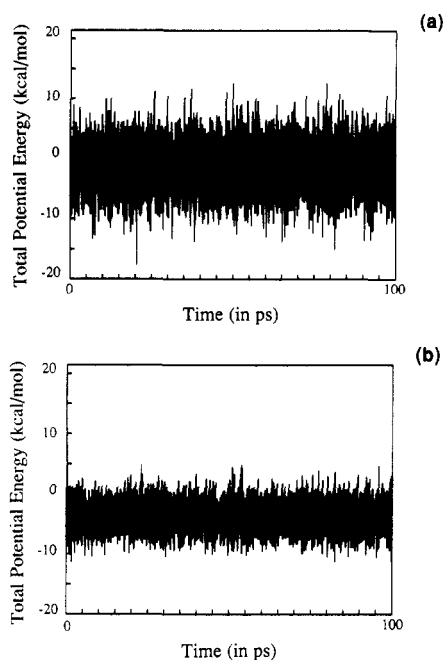

Figure 12. Total potential energy fluctuation in 100 ps (a) when the rotational motions are suppressed, and (b) when the translational motions are suppressed in the MD calculation. Averaged over 20 fs (eq 7 with $\Delta t = 10$ fs); for the 64 water molecular system with TIPS2 potential; $T = 298$ K.

Raman spectrum measured by Walrafen et al.[90] They fitted the baseline intensity of the Raman scattering I_c for the frequency 20–4500 cm^{-1} by a power law, $I_c = k/\omega^\alpha$ ($\alpha = 1.2$–1.3) and for the wider frequency range 0.6–6000 cm^{-1} by a Gaussian logarithmic funciton, $y = A \exp(-Bx^2)$ where $y = \ln I_c$ and $x = \ln (1 + \omega)$; $\ln I_c = A \exp\{-B[\ln(1 + \omega)]^2\}$. This Gaussian function is chosen to yield a finite intensity at very low frequency $\omega < 1$ cm^{-1}. This spectrum can also be divided into three parts; a power law region $\omega > 5$–20 cm^{-1}, a near white noise region $\omega < 3$ cm^{-1}, and a transition region in between. This is then very similar to the above potential energy fluctuation spectrum in the inherent structures[96] with $\alpha = 1.3$ and $f_c = 1$–1.5 cm^{-1}.

A Lorentzian functional form was assigned to this low-frequency component ($\omega < 250$ cm^{-1}) by Mizoguchi et al.[92] They subtracted broad vibrational bands around 60 and 180 cm^{-1} from the total scattering spectrum,
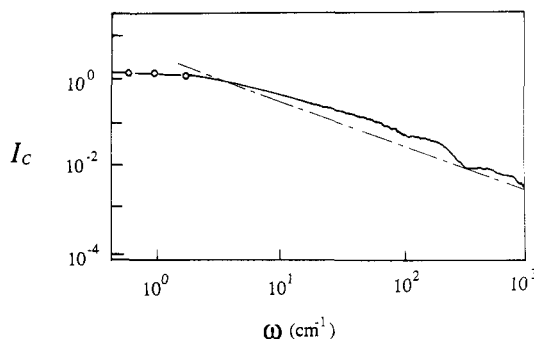

Figure 13. A schematic diagram of Stokes Raman spectrum intensity I_c of liquid water in the frequency range $\omega = 0.6$–1000 cm^{-1}. The plot is of ln I_c versus ln ω. A dashed line is arbitrarily drawn for eye guide. Redrawn from the data of Figure 11 in ref 90. See the original figure in the reference for details.

and concluded that the remaining relaxation mode is of a simple Debye type (Lorentzian); $I_c = 1/\omega^\alpha$ with $\alpha = 0$ in the low frequency ($\omega < 5$ cm^{-1}) and $\alpha = 2$ in the high frequency ($\omega > 40$ cm^{-1}). They also showed that the width Γ ($= 1/\omega\tau$) of this Lorentzian curve increases as the temperature T decreases, following the Curie–Weiss law:

$$\tau = \tau_0 \frac{T-T_c}{T_c}$$

for $T = 263$–368 K with $T_c = 240$ K in heavy water, and with $T_c = 225$ K (but with slight deviation from this equation) in light water. These T_c values correspond to the temperature of the spinodal instability at normal pressure, $P = 1$ atm.

Many other functional forms have been proposed to fit the low-frequency spectrum of liquid water by many other authors; for example, its ω dependence for 0–50 cm^{-1} is fitted by Montrose et al.[100] with two Lorentzians and one exponential. They indicated that the most intensive component in the spectrum arises from the hydrogen bond breaking dynamics. Mazzacurati et al.[94] performed an MD calculation using a polarizability expansion and ascribed the main contribution of the low-frequency spectrum to a dipole-induced-dipole collision-induced element, not necessarily to the hydrogen bond breaking. Mizoguchi et al.[92] have assumed that the long-time hydrogen-bond network rearrangement is the source of this low-frequency component. It is known that clear assignments of functional forms to low-frequency spectra are often difficult. For example, a power spectrum of the intermittent dynamics is known to yield a power law dependence of $I = I/\omega^\alpha$ with the exponent of $\alpha = 2.0$ in all frequency except very low frequency,[97] where it becomes a white noise, $\alpha = 0.0$. This frequency dependence is hard to distinguish from a Debye relaxation case, whose power spectrum yields a white noise in low frequency, the $1/\omega^2$ dependence in the high frequency, and a transition in between. More detailed and careful analyses are thus needed to connect the experimental data and theoretical prediction.

C. Dielectric Relaxation

The dielectric relaxation is a measure of the hydrogen-bond rearrangement dynamics. It is experimentally well established that the dielectric relaxation of liquid

water yields near single exponential decay (i.e., of the Debye type) with the relaxation time τ_1 = 8–9 ps (~17 Ghz) at room temperature.[31] A Cole–Cole curve of the pure Debye type is obtained except for the very high frequency part. Barthel *et al.*,[101] extending the microwave frequency up to 89 GHz in the permitivity spectrum measurement and also using far-infrared data for ω > 150 GHz, showed that a small additional exponent is needed to explain the high frequency part (>40 GHz) of dielectric relaxation. This additional exponent has a relaxation time of τ_2 = 1.02 ps, which corresponds to the lifetime of an individual hydrogen bond. This Debye-type fluctuation of the dielectric relaxation is quite different from the $1/f$ fluctuation of the total potential energy shown above, although both are related to the global hydrogen-bond rearrangement dynamics. The temperature dependence of the dielectric relaxation τ_1 is non-Arrhenius especially in the supercooled regime. To explain this non-Arrhenius behavior, Salvetti *et al.*[31] used the site percolation model by Stanley *et al.*[12,13]

Neuman[102] and Alper and Levy[103] performed a series of MD calculations and evaluated the dielectric relaxation and the individual dipole relaxation in liquid water using various intermolecular potentials. Anderson *et al.*[104] used a flexible water model, SPC (simple point charge) model, to evaluate these relaxations. It was indeed found for all the models that both relaxations are of the Debye type, except that the higher frequency part yields the resonance-type contribution from the librational motion of molecules. The individual dipole relaxation time is estimated to be about 3 ps at T = 292 K in both TIP4P and MCY and 5 ps in SPC. The calculated dielectric relaxation time of the Debye component τ_D is sensitive to the intermolecular potential parameters; τ_D = 6.3 ps in TIP4P and 11 ps in SPC at T = 293 K, which are in fair agreement with the experimental value τ_1 = 8–9 ps, but τ_D = 3 ps in MCY.

The dielectric relaxation is extremely sensitive to a long-range part of the intermolecular potential.[99] If the Coulomb potential is smoothly truncated between r = 7 and 9 Å, then the total dipole relaxation decay time is reduced from about 6 to 1 ps (in TIPS2) and the decay curve changes from a single exponential (Debye) type to a $1/f$ type, whereas a single dipole relaxation still remains to be near Debye and its relaxation time is almost the same in both the truncated and full Coulomb potentials. Furthermore, our recent calculation for small water molecule clusters, $(H_2O)_n$, shows that the dielectric relaxation in these systems clearly yields nonexponential decay and their power spectra are of a $1/f$ type.[84b,c] These facts indicate that the dielectric relaxation process indeed involves the $1/f$ dynamics (multiple processes) but some kind of "averaging" takes place.[84c] For small systems, the "averaging" might not be sufficient, and both the potential energy fluctuation and the dielectric fluctuation yield $1/f$ type relaxation. But for a large system, the "averaging" is effective and the dielectric relaxation becomes Debye although the energy fluctuation does not, because the total dipole is a vector quantity and the dipole–dipole interaction is long-ranged, while the energy is a scalar and mainly (mechanical) local quantity. This point must be clarified in future investigations. Whether its relaxation is exponential

or nonexponential must depend sensitively on the time scale and the spatial scale of the quantity observed.

D. Supercooled State of Liquid Water

The unique fluctuation of liquid water dynamics arises from the fact that it is the mixture of the hard-sphere-type dynamics which dominate at high temperature and the strongly correlated molecular dynamics constrained by hydrogen bond which dominate at low temperature. Long-time fluctuation in liquid water is the reflex of the latter motion. As the temperature decreases, the hydrogen-bond rearrangement slows down, and the thermodynamic quantities exhibit some singular behavior, yielding divergence at T_s as

$$X = A\left|\frac{T}{T_s}-1\right|^{\gamma} + B \qquad (16)$$

An excellent review of the supercooled water was given by Angell[7a,b] and the present status of its research was discussed by Angell[7c] and by Maddox.[105] One of the main focuses on the supercooled water is to understand what kind of singularity is involved. It is suggested that the singular behavior at T_s = 46 °C and P = 1 atm is due to the spinodal instability from the supercooled liquid state to a crystal structure. Speedy and Angell[106] proposed a T–P phase diagram of water with the spinodal line and the homogeneous nucleation line of crystallization. They indicated that the spinodal line, T_s, of the transition from the superheated state to the vapor is continuously connected with this liquid–crystal spinodal line in low temperature by going through the negative pressure region (the reentry of the spinodal line), and therefore the heat capacity C_p divergences have the same exponents γ in both the superheated state transition and in the supercooled state transition.[32–33,106] It should be mentioned that no glass transition intervenes before the homogeneous nucleation of crystallization to an ice structure takes place.

Angell pointed out[7b] that earlier models of water, such as Rice's random network model[2,11] and Stanley's percolation model,[12,13] cannot predict this singularity. The percolation model with random hydrogen bond distribution does not account for long-range correlation in spatial distribution of low-density species, and thus cannot predict a true singularity. Stillinger[16a] tried to explain this singularity by proposing a model in which bulky species of polyhedra increase as the temperature decreases. Speedy[107] imposed the cooperative element in polyhedra association by postulating a self-replication mechanism of pentagons. His model indeed yields the thermodynamic singularity.

It should be mentioned, however, that Poole *et al.*[34a] have performed MD calculation on the phase behavior of supercooled water by using the ST2 potential. They found that the reentry of spinodal line from the negative to positive pressure region does not take place in the low-temperature region that they studied. The recent X-ray scattering investigation of water in range down to −24 °C by Ludwig and co-workers[34b] also shows no evidence for an imminent spinodal type instability.

On the other hand, Sasai[108,109] has calculated the grand canonical partition function of water by constructing the Hamiltonian of the hydrogen network in a lattice gas model (a gel model) and applying the field theo-

retical technique to sum over all topologically possible network patterns.[110] His field theoretical lattice model was shown to yield the reentrance of spinodal line and reproduce the cooperative fluctuations of the hydrogen-bond network.[108] The recent work by Sastry et al.[111] using the a lattice model has also demonstrated the reentrance of the spinodal line, but it did not yield the true divergence at the liquid–solid spinodal at least in the approximation level they used. Further systematic theoretical and experimental studies are required to completely clarify what is the phase behavior of the supercooled water. The studies for the dynamical behavior of the supercooled water based on the firm theoretical models are also required.

VII. Chemical Reaction. Energy Dissipation Mechanism In Liquid Water

Recently great progress has been made in understanding the detailed mechanism of chemical reactions in liquids. Thermally activated barrier crossing reactions,[112–115] electron and proton transfer reactions,[116–117] solvated electron relaxation,[118–120] vibrational relaxation, electric relaxation and solvation processes in photoinduced chemical reactions in solutions[121–125] have been extensively studied. The general consensus obtained so far by these studies is that the solvent response to chemical reaction dynamics can be described within the linear response theory.[126–128] This might be attributed to the fact that a chemical reaction is "one dimensional", changing from a reactant to a product along a reaction coordinate. Solvent dynamics essentially acts orthogonal to the reaction and its effect can be averaged. The reactions studied so far were for relatively large size solute molecules and/or long-range solute–solvent interactions. If the reactions in polar solvents involve electric polarization like many photochemical reactions, polar solvent molecules absorb excess energy as bulk through long-range Coulomb interactions. Amount of energy absorbed by each solvent molecule is small and the solvent behaves as the linear response theory predicts. A polar solvent yields a very quick response to the polarity change of a solute through the solvent "inertia" term in the photoinduced solvation dynamics and this inertia contribution takes into account the most part (80–90%) of the Stokes relaxation, as experimentally found by Rothenthal et al.[129] and theoretically shown by Maroncelli et al.,[130] Fleming and Wolynes,[131] Ando and Kato,[117b] and Cho et al.[132] It should be mentioned that the list of the references here is far from complete, we here list only those related to the fast energy relaxation in liquid water.

Ohmine[125] made an MD analysis for vibrational energy dissipation of a photoexcited molecule in liquid water and compared it with that in liquid Ar. It was found in liquid water that energy transfer from an vibrationally exited molecule to the solvent molecules is very fast and that the transferred excess energy to the solvent molecules surrounding the solute is quickly distributed to other solvent molecules. A similar fast energy transfer and fast heat conduction have been found in many other reactions in liquid water. For example, Rossky and co-workers[120a–e] theoretically predicted that time required for a free electron to decay into a solvated state, releasing large excess energy, is

in the sub-picosecond range, which was in close agreement with experimental values.[118,119] The ultrafast spectroscopic studies of Migus et al.[118] and by Eisenthal and co-workers[119] have observed that the first relaxation process to the "precursor excited state" takes about 0.1–0.2 ps and the next relaxation to the fully solvated ground state required 0.24–0.55 ps.[121b] This fast hydration dynamics is the subject of current intensive theoretical and experimental investigations. The same process takes much longer time in alcohol solutions, about 10 ps observed experimentally.[133,134] The rapid electron relaxation in water clusters was also predicted.[122] Bader and Chandler[135] showed that solvation dynamics in the charge-transfer reactions in aqueous solutions is also very fast.

Another example of fast relaxation in liquid water is an energy relaxation process from a top of energy barrier (the transition state) to product (or reactant) in S_N2 reactions, investigated by Gertner et al.[112] It was also found to be extremely fast, <1 ps. Whitnell et al.[113] and Levine et al.[115] performed a detailed analysis for the vibrational relaxation mechanism of these reactions in liquid water. The excellent review on this subject is given by Whitnell and Wilson.[114] It was found that the energy of reacting molecules is dissipated mainly into the mutual binding potential energies of water molecules. This energy transfer creates "hot spots" in liquid water.[114,115] Using the notion of time reversality of trajectory, they claimed that these hot spots, which exist in liquid water as local energy fluctuations discussed in the present review, are the energy source for the activation of a molecule from a reactant state to the transition state. The activation energy is initially supplied as the mutual translational energy of reacting molecules. It was found[125] that there exists almost no temperature gradient around a hot solute molecule; that is, the excess vibrational energy is distributed very rapidly to the entire solvent due to the existence of strong energy exchange mechanism of the flip–flop-type among water molecules and the large local energy fluctuation.

The energy dissipation mechanism in liquid Ar is quite different from that in liquid water.[114,115,125] The energy dissipation is much slower in liquid Ar than in liquid water for fast reactions, and the excess energy is mainly dissipated into kinetic energies of solvent Ar atoms, not into the intermolecular potential energies of the solvent as in the case of water. A clear threshold behavior is found in the energy-dissipation process in Ar solvent.[109] The dissipation rate is almost zero for small amplitude motion, since the force acting on the Ar atom from the solute molcule cannot become large for the weak Ar–Ar interaction and there is no vibrational–vibrational energy transfer from the fast reacting molecule to the slow Ar–Ar vibrations; they are in off-resonance. But the energy dissipation suddenly starts increasing when the ampliude of reacting molecular motions exceeds a certain threshold value.[109] Then, occasionally occurring hard collisions of solute–solvent induce the energy transfer. The excess energy (heat), transferred from a hot solute molecule to the surrounding Ar atoms, is distributed to other Ar atoms through diffusional processes.[125] So this heat conduction is also slow and the temperature gradient around the solute molecule exists in the Ar solvent.

Water has a wide frequency distribution of the intermolecular (water–water) vibrations and can yield a response even to very fast reactions.[115] Relatively fast energy relaxation occurs even for small amplitude motions. The clear threshold behavior as in liquid Ar is not seen in liquid water. But another kind of threshold behavior might exist in liquid water. When the amplitude of solute motion becomes very large, the energy dissipation rate is amplified by a "nonlinear" response of solvent water. This can occur only in the neutral reactions of small solute molecules, where only a few water molecules surrounding a solute directly absorb the large excess energy and induce a large local rearrangement of the solvation structure. A systematic analysis is needed for the threshold behaviors and the transition of the dissipations mechanisms from a linear to a "nonlinear" response of liquid water.

VIII. Hydration. Aqueous Solutions and Hydrophobic Effects

Hydration of nonpolar solute has a direct bearing on the properties of pure water. In this section, the recent development of theoretical study on hydration of nonpolar solutes will be reviewed.[136,137]

It is well known that a solubility of a nonpolar molecule in water is extremely low. One may expect that the low solubility arises from a weak interaction between water and the solute molecules so that the mixing of nonpolar solute into water is an endothermic process, breaking the strong water–water interaction. Experimental evidences, however, show that a fairly large negative (excess) enthalpy change is accompanied by the hydration.[138-140] Therefore, the immiscibility should be associated with the large negative (excess) entropy change. The hydration process, which is dominated by the entropy term (excess entropy times the temperature) rather than the enthalpy term, is called the hydrophobic hydration. With this entropy-dominant mixing, some anomalous properties observed in pure water are enhanced in aqueous solutions of hydrophobic solutes. The large negative entropy change and exothermicity are usually considered to be associated with a structural enhancement of water around a solute. It is expected that this enhanced structure resembles the clathrate hydrate structure.

When nonpolar solutes are dissolved in water, the solutes tend to associate with each other even in very low concentration, so as to reduce the number of water molecules proximate to solutes. An attractive force acts between two hydrated nonpolar solutes. This is largely a solvent-induced interaction,[138-140] called hydrophobic interaction, and plays a significant role in folding of biological macromolecules and in formation and stabilization of membranes and micelles.[141,142]

The argument above was made primarily on the basis of abundant thermodynamic measurements. The most systematic analysis of the thermodynamic properties has been done by the virial expansion of the solvent in the presence of infinite number of solvent water molecules.[143,144] One of the disadvantages of this analysis is that it is impossible to establish a direct connection between measured virial coefficients and microscopic interactions. This is because there is no clear way of separating the measured values into the direct interaction between solutes and the solvent

induced interaction. Therefore, many theoretical and computational methods have been proposed to explain the hydrophobic effects. It is important to test whether the predictions of various theories agree with experimental data. The most important property for this test is the free energy or entropy of hydration of solutes. The free energy of the hydration is divided formally into two processes: (1) the cavity formation accommodating the solute in water, and (2) introduction of weak but attractive interaction between water and solute. The cavity formation involves the structural reorganization around the solute. The free energy of the cavity formation process seems to increase with increasing the solute size. The attractive interaction also increases as the solute size increases. This contribution, from the interaction, to the free energy has the opposite sign to the contribution from cavity formation. As a result, the attractive interaction blurs the size dependence predicted for the hard-sphere solues and the total free energy of the hydration yields complicated size dependence. For instance, the solubility of noble gases (spherical solutes) increases with the increase of the size, while that of a series of alkane decreases.[139]

A. Scaled Particle Theory

An application of the scaled particle theory was the first attempt to investigate the hydrophobic hydration among the theoretical treatments.[145] In the scaled particle theory, both the water and the solute are treated as hard spheres. Let us consider the reversible work w to create a hard sphere of radius r_0 in water whose hard-sphere radius is r_w and number density is ρ:[146]

$$w = -kT \ln\left(1 - \frac{4\pi\rho r_w^3}{3}\right) +$$
$$4\pi\rho kT \int_0^{r_0} (r_w + r)^2 G(r_w + r) \, dr \quad (17)$$

where the first term corresponds to the free energy to create an infinitesimal size of solute and the second term is the enlarging process to grow the size of this solute from 0 to r_0. The density ρ is treated as an input parameter obtained from the experiment. The effect of water anomaly on the hydration is included in the scaled particle theory through the anomaly in the water density ρ. An approximate form of $G(r)$ can be evaluated in the scaled particle theory: the reversible work to create a macroscopic size of a solute is assumed to have a certain asymptotic form, and this asymptotic form is required to join smoothly to the first term of the eq 17. Pierotti[145] has shown that the free energy evaluated in this method is in good agreement with the experimental data.

A spontaneous cavity formation causes the water structure reorganization around the cavity. If this reorganization makes a significant contribution to the hydrophobic hydration, the free energy of cavity formation is likely to be assessed incorrectly by the scaled particle theory: a much larger positive free energy in cavity formation should be obtained. This theory predicts a positive enthalpy change in the same process, which contradicts the historical view of the hydrophobic hydration. We expect that the water structure enhancement in the vicinity of cavity contributes to the negative enthalpy, which is indeed observed experi-

mentally. The attractive interaction between water and solute, which is missing in this theory, also contributes to the negative enthalpy.

The cavity formation was directly evaluated in the simulation studies by Postma et al.[147] and by Pratt and Pohorille.[82] Pratt and Pohorille obtained $G(r)$ the radial distribution function of the cavity in contact with water and also $G(r)$ in the contact with organic solvents. They found that the cavity size distribution is sharper in water than that in organic neat liquids. In comparison with these simulation results, the scaled particle theory underestimated the contact value of solute–water distribution function. The agreement was improved by the revised scaled-particle theory proposed by Stillinger and Irisa et al.[148]

B. Integral Equations

The integral equation is an approach to assess both hydration and solute–solute interaction. A pioneering work was done by Pratt and Chandler,[149] where thermodynamic and structural properties were obtained only on the basis of the experimental pair correlation function $h_{OO}(r)$. The strategy in the integral equation study is to calculate the pair correlation between water and solute $h_{OS}(r)$ and between solutes, $h_{SS}(r)$, separately with a Percus–Yevick-like approximation in the limit of infinite solute dilution. The solvent-separated association was found to be important as evident from the oscillatory character of $h_{SS}(r)$. Various thermodynamic properties were calculated such as the chemical potential of the apolar solutes, the transfer free energies from nonpolar solvent to water, and the second osmotic coefficients. Most of them were found to be in good agreement with the experimental values. An approximation, different from the typical superposition approximation, was also proposed to calculate the solute conformational equilibria such as a distribution of the dihedral angle of the n-butane. In their later paper,[150] Pratt and Chandler discussed that the attractive force between two solutes is important to evaluate the potential of the mean force between solutes. This method was extended to RISM-like version by taking account of all atomic pair correlation functions. It was found that the solvent-separated hydrophobic interaction is more favorable in some large solutes and that the association is very sensitive to the choice of the approximations in the integral equation.[83,151,152]

C. Simulation of Hydration of Nonpolar Solutes

In order to gain an insight into the three-dimensional structures and the hydrogen-bond network connectivity around a solute, several computer simulation studies were carried out on the solubility of simple hydrophobic solutes in water and on the structure around hydrophobic solutes. Widom's particle insertion method[153] is the simplest way to calculate the excess chemical potential of a solute by the computer simulation. Let us consider a situation where only one solute molecule is dissolved in water. The excess chemical potential of the solute, $\Delta\mu_s$, is written as

$$\Delta\mu_s = -kT \ln \langle \exp(-\beta\phi) \rangle_N \qquad (18)$$

where k is the Boltzmann's constant, T denotes the temperature, $\beta = 1/kT$, and ϕ is the interaction of the

solute with solvents. The number of water is N and the average $\langle \ \rangle_N$ is taken over water configurations in the absence of the solute–water interaction.

In the practical evaluation of the free energy for large and/or nonspherical solutes, the value of $\exp(-\beta\phi)$ is small (i.e., ϕ is large) for most of the configurations, and so the direct evaluation of the free energy using eq 18 is very slowly convergent. Several methods have been proposed to improve the convergence. The thermodynamic integration method was used to evaluate the hydration free energy of large solutes. In this method, the size of the solute gradually increases step by step. At each intermediate reference stage, a free-energy difference is calculated, and then the excess free energy is obtained as the sum of these free-energy difference.[154,155] A more sophisticated method was proposed for the particle insertion of nonspherical molecule and was found to be effective.[156] Swope and Andersen[157] made a systematic study on the solubility for various kinds of spherical solutes by using Hill's methods,[158] in which the excess chemical potentials are evaluated by using adiabatic switching of the coupling parameter of the solute–water interaction. They could reproduce the experimentally observed temperature dependence of solubilities of tested solutes, except for neon.

In addition to the free-energy calculation, the enthalpy calculation or the hydration mixing energy calculation is required in order to make a consistent analysis of hydration. It is also difficult to make a good estimation of this energy in MD or MC simulations. In the simplest form, the hydration energy is given by

$$\Delta U = \langle \Phi_N + \phi \rangle_{N+1} - \langle \Phi_N \rangle_N \qquad (19)$$

where the total potential energy for pure water system is denoted by Φ_N and that for solution by $\Phi_{N+1} = \Phi_N + \phi$, the average $\langle \ \rangle_{N+1}$ is taken over configurations of the system composed of N water molecules plus a solute, and the average $\langle \ \rangle_N$ is over the configuration of the pure water. The straight evaluation of this equation suffers with the severe convergence problem, because $\langle \Phi_N \rangle_{N+1} - \langle \Phi_N \rangle_N$ to be calculated from two different ensembles. Each term independently undergoes a large potential energy fluctuation, which is discussed in the previous sections, and the convergence of each term is slow. Therefore, it is unreliable to evaluate the hydration energy as the difference of these two independent terms. The exothermic hydration by computer simulation study has therefore long been controversial. A new method[159] to evaluate the hydration mixing energy was proposed in which the ensemble average was taken over only a nonperturbed system, by rewriting eq 19, as

$$\Delta U = \langle \phi \rangle_{N+1} + \langle \Phi_N \rangle_{N+1} - \langle \Phi_N \rangle_N$$
$$= \langle \phi \exp(-\beta\phi) \rangle_N / \langle \exp(-\beta\phi) \rangle_N +$$
$$\langle (\Phi_N - \langle \Phi_N \rangle_N) \exp(-\beta\phi) \rangle_N / \langle \exp(-\beta\phi) \rangle_N \qquad (20)$$

This equation converges much faster than eq 19. It was found that the hydration processes are indeed exothermic ($\Delta U < 0$) and entropy dominated. This conclusion is different from that obtained in the previous study.[160]

D. Simulation of Hydrophobic Interactions

Some simulation results on the association of hydrophobic solutes have been reported by MC simula-

Table I. Potential Energy for Water U_w and Methanol U_m for Mixtures at 298.15 K[a]

x_m	U_w (CC)	U_m (CC)	U_w (TP)	U_m (TP)
0.0	-39.51		-42.02	
0.1	-40.12	-36.75	-42.04	-38.95
0.2	-40.29	-36.88	-41.53	-38.29
0.3	-40.49	-36.68	-41.52	-37.66
0.5	-40.63	-35.89	-40.80	-36.32
0.7	-40.32	-35.36	-40.45	-35.33
0.9	-41.05	-34.40	-41.22	-34.46
1.0		-34.10		-34.10

[a] The interactions between unlike molecules are divided equally between individual molecules. The potential energy denoted by U is in kJ mol^{-1}. x_m is the mole fraction of methanol. CC and TP indicate CC and TIP4P potential, respectively.

tions, which agree reasonably with those from the integral equation studies.[161] In addition, Geiger et al.[162] indicated that two neon atoms in water tend to aggregate with each other, but their simulation time (only 8 ps) was too short to give any firm conclusion. In much longer MD simulations by Rapaport and Scheraga[162] or by Watanabe and Andersen,[162] the association of hydrophobic solutes were hardly observed. It was suggested that the degree of association of those solutes depends on the system size[83] and it is sensitive to the periodic boundary condition.[163]

Apart from the convergence problem, a small change in water–water interaction parameter leads to quite different results in the solute–solute pair correlation function and the thermodynamic properties. For example, the origin of exothermic mixing was usually attributed to the strong water–methanol interaction. It was, however, shown that the crucial factor is not only water–solute interaction but also water–water interaction.[164] This was demonstrated in the analysis on the hydration of aliphatic alcohols, which are typical hydrophobic solutes according to Franks' classification. Table I shows that the exothermic mixing of water and methanol arises from two origins. While the potential energy of CC[44] water in mixture is lower than in its pure state, that of the TIP4P[46] water is generally higher than in the pure state. In addition to the pair potential energy between water molecules, the higher body interactions may play a significant role in thermodynamic properties of mixing.

In closing this section, we would like to point out some important problems that need to be solved in future. (1) Conformational equilibria of hydrocarbon chains in water and in other organic solvents have been investigated by many simulations,[165] but the results have not been conclusive. (2) Water structure enhancement plays a dominant role in the hydrophobic hydrations and interaction. According to the simulation and the analysis of the experimental data, the second osmotic coefficients, reflex of the hydrophobic interaction strength, are also very sensitive to relative magnitude of water–solute force and solute–solute attractive force. We need to inquire as to what extent the traditional view of the hydrophobic interaction, which only emphasizes the water structure enhancement, is valid in various systems. Another question is how does the hydrophilic group contribute to the association of polar solutes in aqueous media; Ben-Naim[166] pointed out the importance of the hydrophilic group. Tanaka et al.[167] decomposed the free energy

and evaluated the relative importance between the purely structure enhancement effect and the thermal fluctuation effect in the hydration of various nonpolar solutes. An application of this method to aqueous solutions of polar solutes seems to be useful to answer the above question. (3) According to the traditional interpretation of hydrophobic hydration, the lowering of the water potential energy by the water structure enhancement around solutes is expected to occur in aqueous solutions of apolar gases, but it has not been seen clearly. An investigation on the stability of a clathrate hydrate might serve for better understanding of the origin of this energy change, since the clathrate hydrate structure is expected to be very similar to the hydration structure. The detailed investigation on the potential energy of water and the analysis of the hydrogen bond connectivity in the vicinity of the solute together will enable us to delineate the hydrophobic effects more comprehensively.

IX. Conclusions

In this review, specific attention was focused on the dynamical aspect of water as seen in simulation. It was shown that there exist collective motions and energy fluctuations associated with the hydrogen-bond network rearrangements dynamics in liquid water. The collective motions involve tens of water molecules localized in space. The potential energy fluctuation caused by these collective motions yields $1/f$ noise, which means that the multi-relaxation processes are involved in the dynamics. The slowest fluctuation, reflex of the global hydrogen-bond network rearrangement, is in the order of tens of piseconds, about ten times longer that the individual hydrogen bond lifetime.

It was suggested that these characteristics of liquid water dynamics indeed appear in the experimental data. (1) Raman scattering yields a power law type frequency dependence ($1/\omega^\alpha$) of the very low frequency component. (2) The coherent inelastic neutron scattering yields the collective motion of the water molecules in the length of 10–20 Å. It is known in dynamics of glassy materials that a different experimental technique (Raman scattering, the dielectric relaxation measurement, and the light scattering, etc.) yields a different relaxation time, depending on what kind of mode is measured by each technique. The liquid water in ambient condition is fluid but has many properties of the glassy states associated with multiple hydrogen-bond network structures. So the experimental observations with the variety of relaxation times are expected. For some physical observables such as the dielectric relaxation, however, the delicate balance of cancellation must exist so that their relaxation becomes a simple Debye.

The inherent structure analysis is a powerful tool to investigate the dynamics of many-particle systems, when local structure of the potential energy surface around potential energy minima (inherent structures) is important. Fundamental structures, their transitions, reaction coordinates, and normal modes are well defined by using the inherent structures. Hydrogen-bonding structures are also defined without ambiguity of conformational distortions. The inherent structure analysis has also been successfully applied to calculate the free energies of clusters and to predict the "melting" transitions. The inherent analysis needs to be extended

to deal with the global feature of potential energy surfaces in order to understand the mechanism of long-time fluctuation and the transitions in liquid dynamics. New methods need to be developed to investigate the higher energy part of the potential energy surface where anharmonicity and mode mixing are important.

There is a need to analyze more thoroughly the hydrogen-bond network multiplicity and its relation to the global potential energy surface structure for liquid water and to explain why the homogeneous nucleation of the crystallization takes place without intervention of the glass transition. There is also a need to find out how the long range structural order in the hydrogen bond network couples with local thermal kinetic disordering and how the collective motion and energy fluctuation arise from this coupling as the temperature increases. A time-dependent analysis using a model Hamiltonian of a gel network (hydrogen network) must shed light on their coupling mechanism. The extension in a graph theory of network will be useful to classify the hydrogen network patterns and define the similarity among the network structures in different instances in order to extract a backbone network structure, if it exists, which controls the overall dynamics of liquid water.

The present status of the theoretical studies on the hydrophobic effects were also reviewed. The scaled particle theory, integral equations, and computer simulations were discussed. The simple picture for the hydration of nonpolar solutes expected from experiment was confirmed; it is the entropy dominant process. It was also shown that an association of solutes, known as hydrophobic interaction, was very sensitive to the balance between the attractive interaction of water–solute and that of the solute–solute. This means that the traditional view of hydrophobic effects is crude. It is important to establish a new picture of the hydrophobic effects by taking into account not only an enhancement of water structure but also the factor that originated from attractive interactions. The significance of the hydrophobic effects in folding biological macromolecules and in stabilizing micelles and membranes cannot be clarified until the role of hydrophilic and hydrophobic groups becomes clear.

References

(1) Eisenberg, D.; Kauzmann, W. *The Structure and Properties of Water*; Oxford University: London, 1969.

(2) Sceats, M. G.; Rice, S. A. *Water, a Comprehesive Treatise*; Franks, F., Ed.; Plenum: New York, 1982; Vol. 7, p 13, and references therein.

(3) *Water, a Comprehensive Treatise*; Franks, F., Ed.; Plenum: New York, 1972–1982; Vols 1–7.

(4) *Hydrogen-Bonded Liquids*; Dore, J. C., Teixeira, J., Eds.; Kluwer Academic Publishers: Dordrecht, The Netherlands, 1991.

(5) *Water & Aqueous Solutions*; Neilson, G. W., Enderby, J. E., Eds.; Adam Hilger Press: Bristol, 1986.

(6) *Water Science Reviews*; Franks, F., Ed.; Cambridge Press: Cambridge, 1985–1990; Vols. 1–5.

(7) (a) C. A. Angell, In *Water: A Comprehensive Treatise*; Franks, F., Ed.; Plenum: New York, 1982; Vol. 7, p 1. (b) Angell, C. A. *Ann. Rev. Phys. Chem.* **1983**, *34*, 593. (c) Angell, C. A. *Nature* (London) **1988**, *331*, 206.

(8) Geiger, A.; P. Mausbach; P. In *Hydrogen-Bonded Liquids*; Dore, J. C., Teixeira, J., Ed.; Kluwer Academic Publishers: Dordrecht, 1991; p 171.

(9) Frank, H. S.; Wen, W. Y. *Discuss. Faraday Soc.* **1957**, *24*, 133.

(10) (a) Pople, J. A. *Proc. R. Soc. London* **1950**, *A202*, 323. (b) Pople, J. A. *Proc. R. Soc. London* **1951**, *A205*, 163.

(11) (a) Belch, A.; Rice, S. A.; Sceats, M. G. *Chem. Phys. Lett.* **1981**, *77*, 455. (b) Belch, A.; Rice, S. A. *J. Chem. Phys.* **1987**, *86*, 5676.

(12) Stanley, H. E.; Teixeira, J. *J. Chem. Phys.* **1980**, *73*, 3404.

(13) (a) Blumberg, R. L.; G., Shliefer; Stanley, H. E. *J. Phys.* **1980**, *A13*, L147. (b) Geiger, A.; Stanley, H. E. *Phys. Rev. Lett.* **1982**, *49*, 1749. (c) Blumberg, R. L.; Stanley, H. E.; Geiger, A.; Mausbach, P. *J. Chem. Phys.* **1984**, *80*, 5230.

(14) Rahman, A.; Stillinger, F. H. *J. Chem. Phys.* **1971**, *55*, 3336.

(15) (a) Stillinger, F. H.; Weber, T. A. *Phys. Rev.* **1982**, *A25*, 97. (b) Stillinger, F. H.; Weber, T. A. *Phys. Rev.* **1983**, *A28*, 2408.

(16) (a) Stillinger, F. H.; Weber, T. A. *J. Phys. Chem.* **1983**, *87*, 2833. (b) Stillinger, F. H.; Weber, T. A. *Science* **1984**, *225*, 983.

(17) Ohmine, I.; Tanaka, H.; Wolynes, P. G. *J. Chem. Phys.* **1988**, *89*, 5852.

(18) Tanaka, H.; Ohmine, I. *J. Chem. Phys.* **1989**, *91*, 6318.

(19) Ohmine, I.; Tanaka, H. *J. Chem. Phys.* **1990**, *93*, 8138.

(20) (a) Amar, F. G.; Berry, R. S. *J. Chem. Phys.* **1986**, *85*, 5943. (b) Berry, R. S.; Beck, T. L.; Davis, H. L.; Jellinek, J. *Adv. Chem. Phys.* **1988**, *70* (Part 2), 75 and references therein. (c) Beck, T. L.; Jellinek, J.; Berry, R. S. *J. Chem. Phys.* **1987**, *87*, 545. (d) Beck, T. L.; Berry, R. S. *J. Chem. Phys.* **1988**, *88*, 3910. (e) Rose, J. P.; Berry, R. S. *J. Chem. Phys.* **1992**, *96*, 517.

(21) (a) Wales, D. J.; Berry, R. S. *J. Chem. Phys.* **1990**, *92*, 4283. (b) Walse, D. J. *Mol. Phys.*, in press. (c) Wales, D. J. *J. Am. Chem. Soc.* **1990**, *112*, 7908. (d) Wales, D. J. *Mol. Phys.* **1991**, *74*, 1.

(22) Cheng, H.-P.; Berry, R. S. *Phys. Rev.* **1992**, *A45*, 7969.

(23) Labastie, P.; Whetten, R. L. *Phys. Rev. Lett.* **1990**, *65*, 1567.

(24) (a) Nemethy, G.; Scherage, H. A. *J. Chem. Phys.* **1962**, *36*, 3382, 3401. (b) Hagler, A. T.; Scheraga, H. A.; Nemethy, G. *J. Phys. Chem.* **1972**, *76*, 3229.

(25) Bernal, J. D.; Fowler, R. H. *J. Chem. Phys.* **1933**, *1*, 515.

(26) (a) Stillinger, F. H.; Rahman, A. *J. Chem. Phys.* **1974**, *60*, 1545. (b) Stillinger, F. H.; Rahman, A. *J. Chem. Phys.* **1975**, *61*, 4973. (c) Stillinger, F. H.; Rahman, A. *J. Chem. Phys.* **1972**, *57*, 1281.

(27) (a) Kataoka, Y.; Hamada, H.; Nose, S.; Yamamoto, T. *J. Chem. Phys.* **1982**, *77*, 5699. (b) Okazaki, K.; Nose, S.; Kataoka, Y.; Yamamoto, T. *J. Chem. Phys.* **1981**, *75*, 5864.

(28) (a) Oguni, M.; Angell, C. A. *J. Chem. Phys.* **1980**, *73*, 1948. (b) Kanno, H.; Angell, C. A. *J. Chem. Phys.* **1979**, *70*, 4008. (c) Sugisaki, M.; Suga H.; Seki, S. *Bull. Chem. Soc. Jpn.* **1968**, *41*, 2594.

(29) Stauffer, D. *Introduction to Percolation Theory*; Tayler and Francis: London, 1985.

(30) Stanely, H. E. *J. Phys.* **1979**, *A12*, L329.

(31) (a) Bertolini, D.; Cassettrari, M.; Salvetti, G. *J. Chem. Phys.* **1982**, *76*, 3285. (b) Salvetti, G. In *Hydrogen-Bonded Liquids*; Dore, J. C., Teixeira, J., Eds.; Kluwer Academic Publishers: Dordrecht, The Netherlands, 1991; p 369. (c) Bertollini, D.; Cassettrari, M.; Ferrario M.; Grigolini, P.; Salvetti, G. *Adv. Chem. Phys.* **1985**, *62*, 277. (d) Bertolini, D.; Cassettari, M.; Ferrario, M.; Grigolini, P.; Salvetti, G.; Tani, A. *J. Chem. Phys.* **1989**, *91*, 1179.

(32) (a) Prielmeier, F. X.; Lang, E. W.; Speedy, R. J.; Lüdemann, H.-D., *Phys. Rev. Lett.* **1987**, *59*, 1128. (b) Taborek, P.; Kleiman, R. N.; Bishop, D. J. *Phys. Rev.* **1986**, *B34*, 1835. (c) Walrafen, G. E.; Chu, Y. C. *J. Phys. Chem.* **1992**, *96*, 3840.

(33) (a) Speedy, R. J. *J. Phys. Chem.* **1982**, *86*, 982. (b) Speedy, R. J. *J. Phys. Chem.* **1982**, *86*, 3002. (c) Speedy, R. J. *J. Phys. Chem.* **1987**, *91*, 3354. (d) Speedy, R. J. *J. Phys. Chem.* **1984**, *88*, 3364. (e) Speedy, R. J.; Mezei, M. *J. Phys. Chem.* **1985**, *89*, 171.

(34) (a) Poole, P. H.; Sciortino, F.; Essmann, U.; Stanley, H. E. *Nature* **1990**, *360*, 323. (b) Xie, Y.; Ludwig, K. F.; Morales, G.; Hare, D. E.; Sorensen, C. M. *Phys. Rev. Lett.* **1993**, *71*, 2050.

(35) Allen, P. M.; Tildesley, D. J. *Computer Simulation of Liquids*; Oxford: New York, 1987.

(36) Goldstein, H. *Classical Mechanics*, 2nd ed.; Addison Wesley: Reading, MA, 1980.

(37) Gear, C. W. *The numerical initial value problem of ordinary differential equations*; Prentice Hall: Englewood Cliffs, 1971.

(38) Evans, D. J.; Murad, S. *Mol. Phys.* **1977**, *34*, 327.

(39) (a) Ewald, P. *Ann. Phys.* **1921**, *64*, 253. (b) Nijboer, B. R. A.; De Wette, F. W. *Physica* **1957**, *23*, 309. (c) Ceperly, D. *Phys. Rev.* **1978**, *B18*, 3126.

(40) (a) Hankins, D.; Moskowitz, J. W.; Stillinger, F. H. *J. Chem. Phys.* **1970**, *53*, 4544. (b) Clementi, E.; Kolos, W.; Lie, G. C.; Ranghino, G. *Int. J. Quant. Chem.* **1980**, *17*, 377. (c) Gellatly, B. J.; Quinn, J. E.; Barens, P.; Finney, J. L. *Mol. Phys.* **1983**, *50*, 948.

(41) Wojcik, M.; Clementi, E. *J. Chem. Phys.* **1986**, *84*, 5970.

(42) (a) Reimers, J. R. *Chem. Phys.* **1984**, *91*, 201. (b) Lybrand, T. P.; Kollman, P. A. *J. Chem. Phys.* **1985**, *83*, 2923. (c) Sprik, M.; Klein, M. L. *J. Chem. Phys.* **1988**, *89*, 7556. (d) Kuwajima, S.; Warshel, A. *J. Phys. Chem.* **1990**, *94*, 460. (e) Cieplack, P.; Kollman, P. A. *J. Chem. Phys.* **1990**, *92*, 6755. (f) Straatsma, T. P.; McCammon, J. A. *Mol. Simulat.* **1990**, *5*, 181. (g) Watanabe, K.; Klein, M. L. *Chem. Phys.* **1989**, *131*, 57. (h) Niesar, U.; Corongiu, G.; Clementi, E. *J. Chem. Phys.* **1990**, *92*, 6755. (i) Zhu, Z. B.; Zhu, J. B.; Singh, S.; Robinson, G. W. *J. Phys. Chem.* **1991**, *95*, 6211.

(43) Ben-Naim, A.; Stillinger, F. H. In *Structure and Transport Process in Water and Aqueous Solutions*; Horne, R. B., Ed.; (Wiley Interscience: New York, 1972; p 295.

(44) (a) Matsuoka, O.; Clementi, E.; Yoshimine, M. *J. Chem. Phys.* **1976**, *64*, 1351. (b) Clementi, E.; Habitz, P. *J. Phys. Chem.* **1983**, *87*, 2815. (c) Carravetta, V.; Clementi, E. *J. Chem. Phys.* **1984**, *81*, 2646.

(45) (a) Berendsen, H. J. C.; Postma, J. P. M.; van Gunsteren, W. F.; Hermans, J. In *Intermolecular Forces*; Pullman, B., Ed.; Reidel: Dordrecht, Holland, 1981. (b) Berendsen, H. J. C.; Grigera, J. R.; van Gunsteren, W. F. *J. Phys. Chem.* **1987**, *91*, 6269.

(46) (a) Jorgensen, W. L. *J. Am. Chem. Soc.* **1981**, *103*, 335. (b) Jorgensen, W. L. *J. Chem. Phys.* **1982**, *77*, 4156. (c) Jorgensen, W. L.; Chandrasekhar, J.; Madura, J. D.; Impey, R. W.; Klein, M. L. *J. Chem. Phys.* **1983**, *79*, 926.

(47) Narten, A. H.; Danford, M. D.; Levy, H. A. *Discuss. Faraday Soc.* **1967**, *43*, 97.

(48) (a) Pangali, C. S.; Rao, M.; Berne, B. J. *Computer Modeling of Matter*; Lykos, P., Ed.; American Chemical Society: Washington, DC, 1978; Chapters 2 and 3. (b) Finney, J. L.; Quinn, J. E.; Baum, J. O. *Water Science Review* Franks, F., Ed.; Cambridge University Press: Cambridge, 1985; Vol. 1, Chapter 2.

(49) (a) Morse, M. D.; Rice, S. A. *J. Chem. Phys.* **1981**, *74*, 6514. (b) Morse, M. D.; Rice, S. A. *J. Chem. Phys.* **1982**, *76*, 650. (c) Nielson, G.; Rice, S. A. *J. Chem. Phys.* **1984**, *80*, 4456. (d) Nielson, G.; Townsend, R. M.; Rice, S. A. *J. Chem. Phys.* **1984**, *81*, 5288.

(50) Tse, J. S.; Klein, M. L.; McDonald, I. R. *J. Chem. Phys.* **1984**, *81*, 6124.

(51) Yoon, B. J.; Morokuma, K.; Davidson, E. R. *J. Chem. Phys.* **1985**, *83*, 1223.

(52) (a) Rahman, A.; Stillinger, F. H.; Lemberg, H. L. *J. Chem. Phys.* **1975**, *63*, 5223. (b) Stillinger, F. H.; Rahman, A. *J. Chem. Phys.* **1978**, *68*, 666.

(53) (a) Sciortino, F.; Geiger, A.; Stanley, H. E. *Phys. Rev. Lett.* **1990**, *65*, 3452. (b) Sciortino, F.; Geiger, A.; Stanley, H. E. *Nature* **1991**, *354*, 218. (c) Sciortino, F.; Geiger, A.; Stanley, H. E. *J. Chem. Phys.* **1992**, *96*, 3857.

(54) Fletcher, R. *Practical Methods of Optimization; Unconstrained Optimization*; Wiley: New York, 1980; Vol. 1.

(55) Tanaka, H.; Nakanishi, K. *Mol. Simulat.* **1991**, *6*, 311.

(56) Kirkpatrick, S.; Gelatt, C. D.; Vecchi, M. P. *Science* **1983**, *220*, 671.

(57) Fisher, K. H.; Hertz, J. A. *Spin Glasses*, Cambridge University Press: Cambridge, 1991.

(58) Hirata, F.; Rossky, P. J. *J. Chem. Phys.* **1981**, *74*, 6867.

(59) Tanaka, H.; Ohmine, I. *J. Chem. Phys.* **1987**, *87*, 6128.

(60) (a) Geiger, A.; Stillinger, F. H.; Rahman, A. *J. Chem. Phys.* **1979**, *70*, 4185. (b) Speedy, R. J.; Madura, J. D.; Jorgensen, W. L. *J. Phys. Chem.* **1987**, *91*, 909. (c) Alstrøm, P.; Sciortino, F. *Phys. Rev. Lett.* **1990**, *65*, 2885.

(61) (a) Sciortino, F.; Fornili, S. L. *J. Chem. Phys.* **1989**, *90*, 2786. (b) Sciortino, F.; Poole, P. H.; Stanley, H. E.; Havline, S. *Phys. Rev. Lett.* **1990**, *64*, 1686.

(62) Marshall, W.; Lovesey, S. W. *Thermal Neutron Scattering*; Oxford University Press: 1971.

(63) (a) Teixeira, J.; Bellissent-Funel, M.-C.; Chen, S. H.; Dianoux, A. J. *Phys. Rev.* **1985**, *A31*, 1913. (b) Teixeira, J.; Bellissent-Funel, M.-C.; Chen, S. H. *J. Phys.; Condens. Matter* **1990**, *2*, SA105.

(64) Teixeira, J.; Bellissent-Funel, M.-C.; Chen, S. H.; Dorner, B. *Phys. Rev. Lett.* **1985**, *54*, 2681.

(65) Chen, S. H. In *Proc. NATO ASI on Hydrogen-Bonded Liquids*; Dore, J. C., Teixeira, J., Eds.; Kluwer: Dordrecht, 1991; p 289 and references therein.

(66) (a) Bellissent-Funel, M.-C.; Teixiera, J. *J. Mol. Struct.* **1991**, *250*, 213. (b) Teixiera, J.; Bellissent-Funel, M.-C.; Chen, S. H.; Dorner, B. In *Water and Aqueous Solutions*; Neilson, G. W., Enderby, J. E., Eds.; Adam Hilger Press: Bristol, 1986; p 99.

(67) Ricci, M. A.; Rocca, D.; Ruocco, G.; Vallauri, R. *Phy. Rev. A* **1989**, *40*, 7226 and references therein.

(68) Deriu, A.; Cavatorta, F.; Cabrini, D.; Carlile, C. J.; Middendorf, H. D. Preprint titled *Water Dynamics in Biopolymer Gels by Quasi-elastic Neutron Scattering*.

(69) Muller, K. *Angew. Chem., Int. Ed. Engl.* **1980**, *19*, 1 and the references therein.

(70) Cerjan, C. J.; Miller, W. H. *J. Chem. Phys.* **1981**, *75*, 2800.

(71) (a) Hoffman, D. K.; Nord, R. S.; Ruedenberg, K. *Theor. Chim. Acta* **1986**, *69*, 265. (b) Valtazanos, P.; Ruedenberg, K. *Theor. Chim. Acta* **1986**, *69*, 281.

(72) Elber, R.; Karplus, M. *Chem. Phys. Lett.* **1987**, *139*, 375.

(73) McIver, J. W.; Komornicki, A. *J. Am. Chem. Soc.* **1972**, *94*, 2625.

(74) Fukui, K.; Kato, S.; Fujimoto, H. *J. Am. Chem. Soc.* **1975**, *97*, 1. Kato, S.; Fukui, K. *J. Am. Chem. Soc.* **1976**, *98*, 6395.

(75) Ulitsky, A.; Elber, R. *J. Chem. Phys.* **1990**, *92*, 1510. Choi, C.; Elber, R. *J. Chem. Phys.* **1991**, *94*, 751.

(76) Czerminski, R.; Elber, R. *Int. J. Quantum. Chem. Symp.* **1990**, *24*, 167.

(77) Nguyen, D. T.; Case, D. A. *J. Phys. Chem.* **1985**, *89*, 4020.

(78) (a) Wales, D. J.; Berry, R. S. *J. Chem. Phys.* **1990**, *92*, 4283. (b) Davis, H. L.; Wales, D. J.; Berry, R. S. *J. Chem. Phys.* **1990**, *92*, 4308. (c) Wales, D. J. *J. Chem. Phys.* **1989**, *91*, 7002. (d) Wales, D. J. *Chem. Phys. Lett.* **1990**, *166*, 419.

(79) Wales, D. *J. Chem. Soc., Faraday Trans.* **1990**, *86*, 3505.

(80) Shida, N.; Almlof, J. E.; Barbara, P. E. *Theor. Chim. Acta* **1989**, *76*, 7.

(81) Grest, G. S.; Cohen, M. H. *Adv. Chem. Phys.* **1981**, *48*, 455 and references therein.

(82) (a) Pohorille, A.; Pratt, L. R. *J. Am. Chem. Soc.* **1990**, *112*, 5066. (b) Pohorille, A.; Pratt, L. R. *Proc. Natl. Acad. Sci. U.S.A.* **1992**, *89*, 2995.

(83) Tanaka, H. *J. Chem. Phys.* **1987**, *86*, 1512.

(84) (a) Wales, D.; Ohmine, I. *J. Chem. Phys.* **1993**, *98*, 7245 and 7257. (b) Ohmine, I.; Saito, S.; Wales, D. To be published. (c) Saito, S.; Ohmine, I. To be published.

(85) Geldard, J. F.; Pratt, L. R. *J. Chem. Educ.* **1987**, *64*, 425.

(86) Martin, P. C. In *Measurement and Correlation Functions*; Gordon and Beach: New York, 1968; Chapter B.

(87) Pohorille, A.; Pratt, L. R.; LaViolette, R. A.; Wilson, M. A.; MacElroy, M. A. *J. Chem. Phys.* **1987**, *87*, 6070.

(88) Bright, E.; Decius, J. C.; Cross, P. C. *Molecular Vibrations*; Dover: New York, 1955.

(89) McGinty, D. J. *J. Chem. Phys.* **1973**, *58*, 4733.

(90) Walrafen, G. E.; Hokmabadi, M. S.; Yang, W.-H.; Chu, Y. C.; Monosmith, B. *J. Phys. Chem.* **1989**, *93*, 2909 and references therein.

(91) Walrafen, G. E. In *Hydrogen-Bonded Liquids*; Dore, J. C., Teixeira, J., Eds.; Kluwer Academic Publishers: Dordrecht, The Netherlands, 1991, p 283. (b) Walrafen, G. E.; Hokmabadi, M. S.; Chu, Y. C. In *Hydrogen-Bonded Liquids*; Dore, J. C., Teixeira, J., Eds.; Kluwer Academic Publishers: Doredrecht, The Netherlands, 1993; p 261. (c) Walrafen, G. E.; Fisher, M. S.; Hokmabadi, M. S.; Yang, W.-H. *J. Chem. Phys.* **1986**, *85*, 6970.

(92) Mizoguchi, K.; Hori, Y.; Tominaga, Y. *J. Chem. Phys.* **1992**, *97*, 1961.

(93) Kirshnamurthy, S.; Bansil, R.; Waife-Akenten, J. *J. Chem. Phys.* **1983**, *79*, 5863.

(94) (a) Mazzacurati, V.; Ricci, M. A.; Ruocco, G.; Sampoli, M. *Chem. Phys. Lett.* **1989**, *159*, 383. (b) Mazzacurati, V.; Nucara, A.; Ricci, M. A.; Ruocco, G.; Signorelli, G. *J. Chem. Phys.* **1990**, *93*, 7767.

(95) Madden, P. A.; Impey, R. W. *Chem. Phys. Lett.* **1986**, *123*, 502.

(96) Sasai, M.; Ohmine, I.; Ramaswamy, R. *J. Chem. Phys.* **1992**, *96*, 3045.

(97) (a) Weissman, M. B. *Rev. Mod. Phys.* **1988**, *60*, 573. (b) Dutta, P.; Horn, P. M. *Rev. Mod. Phys.* **1981**, *53*, 497.

(98) Aizawa, Y.; Kikuchi, Y.; Harayama, T.; Yamamoto, K.; Ota, M.; Tanaka, T. *Proc. Theor. Phys. Suppl.* **1989**, *36*, 985.

(99) Ohmine, I. In *Proc. EBSA Conference, Palermo, Italy*, edited by Palmer, *Ital. Phys. Soc.* **1993**, *43*, 7.

(100) Montrose, C. J.; Bucaro, J. A.; Marshall-Coakley, J.; Litovitz, T. A. *J. Chem. Phys.* **1974**, *60*, 5025.

(101) Barthel, J.; Bachhuber, K.; Bunchner, R.; Hetzenauer, H. *Chem. Phys. Lett.* **1990**, *165*, 369.

(102) (a) Neuman, M. *J. Chem. Phys.* **1985**, *82*, 5663. (b) Neuman, M. *J. Chem. Phys.* **1988**, *85*, 1567 and the references therein.

(103) Alper, H. E.; Levy, R. M. *J. Chem. Phys.* **1989**, *91*, 1242.

(104) Anderson, J.; Ullo, J. J.; Yip, S., *J. Chem. Phys.* **1987**, *87*, 1726.

(105) Maddox, J. *Nature* **1987**, *326*, 823.

(106) Speedy, R. J.; Angell, C. A. *J. Chem. Phys.* **1976**, *65*, 851.

(107) Speedy, R. J. *J. Phys. Chem.* **1984**, *88*, 3364.

(108) Sasai, M. *J. Chem. Phys.* **1990**, *93*, 7329.

(109) Ohmine, I.; Sasai, M. *Prog. Theor. Phys. Suppl.* **1991**, *103*, 61.

(110) (a) De Gennes, P. G. *Scaling Concepts in Polymer Physics*; Cornell University: Ithaca, NY, 1979; *Phys. Lett.* **1972**, *38A*, 339. (b) Des Cloizeaux, J. *J. Phys.* **1975**, *36*, 281. (c) Lubensky, T. C.; Isaacson, J. *Phys. Rev. Lett.* **1978**, *41*, 829. (d) Lubensky, T. C.; Isaacson, J. *Phys. Rev.* **1979**, *A20*, 2130. (e) Lubensky, T. C.; Isaacson, J. *J. Phys.* **1981**, *42*, 175.

(111) Sastry, S.; Sciortino, F.; Stanley, H. E. *J. Chem. Phys.* **1993**, *98*, 9863.

(112) (a) Bergsma, J. P.; Gertner, B. J.; Wilson, K. R.; Hynes, J. T. *J. Chem. Phys.* **1987**, *86*, 1356. (b) Gertner, B. J.; Bergsma, J. P.; Wilson, K. R.; Lee, S.; Hynes, J. T. *J. Chem. Phys.* **1987**, *86*, 1377. (c) Gertner, B. J.; Wilson, K. R.; Hynes, J. T. *J. Chem. Phys.* **1989**, *90*, 3537. (d) Gartner, B. J.; Whitnell, R. M.; Wilson, K. R.; Hynes, J. T. *J. Am. Chem. Soc.* **1991**, *113*, 74.

(113) (a) Whitnell, R. M.; Wilson, K. R.; Hynes, J. T. *J. Phys. Chem.* 1990, *94*, 8625. (b) Whitnell, R. M.; Wilson, K. R.; Hynes, J. T. *J. Chem. Phys.* 1992, *96*, 5354.

(114) Whitnell, R. M.; Wilson, K. R. *Reviews in Computational Chemistry*; Lipkowitz, K. B., Boyed, D. B., Eds.; VCH: New York, 1993; Vol 4, pp 67–148.

(115) Wilson, K. R.; Levine, R. D. *Chem. Phys. Lett.* 1988, *152*, 435.

(116) (a) Hatano, Y.; Kakitani, T.; Yoshimori, A.; Saito, M.; Mataga, N. *J. Phys. Soc. Jpn.* 1990, *59*, 1104. (b) Carter, E. A.; Hynes, J. T. *J. Phys. Chem.* 1989, *93*, 2184. (c) Carter, E. A.; Hynes, J. T. *J. Chem. Phys.* 1991, *94*, 5961.

(117) (a) Kato, S.; Amatatsu, Y. *J. Chem. Phys.* 1990, *92*, 7241. (b) Ando, K.; Kato, S. *J. Chem. Phys.* 1991, *95*, 5966.

(118) (a) Migus, A.; Gauduel, Y.; Martin, J. L.; Antonetti, A. *Phys. Rev. Lett.* 1987, *58*, 1559. (b) Gauduel, Y.; Pommeret, S.; Migus, A.; Antonetti, A. *J. Phys. Chem.* 1989, *93*, 3880. (c) Gauduel, Y.; Pommeret, S.; Migus, A.; Antonetti, A. 1991, *95*, 533; *Chem. Phys.* 1990, *149*, 1. (d) Gauduel, Y.; Pommeret, S.; Migus, A.; Yamada, N.; Antonetti, A. *J. Am. Chem. Soc.* 1990, *112*, 2925.

(119) (a) Long, F. H.; Lu, H.; Eisenthal, K. B. *Chem. Phys. Lett.* 1989, *160*, 464. (b) Long, F. H.; Lu, H.; Eisenthal, K. B. *J. Chem. Phys.* 1989, *91*, 4413. (c) Long, F. H.; Lu, H.; Eisenthal, K. B. *Phys. Rev. Lett.* 1990, *64*, 1469.

(120) (a) Webster, F. J.; Rossky, P. J.; Friesner, R. A. *Comput. Phys. Commun.* 1991, *63*, 494. (b) Webster, F. J.; Schnitker, J.; Friedrichs, M. S.; Friesner, R. A.; Rossky, P. J. *Phys. Rev. Lett.* 1991, *66*, 3172. (c) Murphrey, T. H.; Rossky, P. J. *J. Chem. Phys.* 1993, *99*, 515. (d) Keszei, E.; Nagy, S.; Murphrey, T. H.; Rossky, P. J. *J. Chem. Phys.* 1993, *99*, 2004 and the references therein. (e) Space, B.; Coker, D. F. *J. Chem. Phys.* 1991, *94*, 1976.

(121) (a) Barbara, P.; Jarzeba, W. *Adv. Photochem.* 1990, *15*, 1 and references therein. (b) Alfano, J. C.; Walhout, P. K.; Kimura, Y.; Barbara, P. F. *J. Chem. Phys.* 1993, *98*, 5996.

(122) (a) Barnett, R. B.; Landeman, U.; Nitzan, A. *J. Chem. Phys.* 1989, *90*, 4413. (b) Barnett, R. B.; Landeman, U.; Nitzan, A. *J. Chem. Phys.* 1989, *91*, 5567. (c) Barnett, R. B.; Landeman, U.; Nitzan, A. *J. Chem. Phys.* 1989, *93*, 6535. (d) Neria, E.; Nitzan, A.; Barnett, R. N.; Landeman, U. *Phys. Rev. Lett.* 1991, *67*, 1011.

(123) (a) Oxtoby, D. W. *Adv. Chem. Phys.* 1981, *47*, 487 and references therein. (b) Diestler, D. J. *Adv. Chem. Phys.* 1980, *42*, 305. (c) Jolly, D. L.; Freasier, B. C.; Nordholm, S. *Chem. Phys.* 1977, *21*, 211; 1977, *25*, 361; 1980, *52*, 269. (d) Nordholm, S.; Jolly, D. L.; Freasier, B. C. *Chem. Phys.* 1977, *23*, 135.

(124) (a) Nesbitt, D. J.; Hynes, J. T. *J. Chem. Phys.* 1982, *77*, 2130. (b) Hynes, J. T.; Kapral, R.; Torrie, G. M. *J. Chem. Phys.* 1980, *72*, 177. (c) Brooks, C. L., III; Balk, M. W.; Adelman, S. A. *J. Chem. Phys.* 1983, *79*, 784. (d) Balk, M. W.; Brooks, C. L.; Adelman, S. A. *J. Chem. Phys.* 1983, *79*, 804.

(125) Ohmine, I. *J. Chem. Phys.* 1986, *85*, 3342.

(126) Yamamoto, T. *J. Chem. Phys.* 1960, *33*, 281.

(127) (a) Hynes, J. T. *Theory of Chemical Reaction Dynamics*; Baer, M., Ed.; Chemical Rubber Company: Florida, 1985; Vol. 4, p 171 and references therein. (b) Groute, R. F.; Hynes, J. T. *J. Chem. Phys.* 1980, *73*, 2715; 1981, *74*, 4465.

(128) (a) Hanggi, P.; Talkner, P.; Borkovec, M. *Rev. Mod. Phys.* 1990, *62*, 251. (b) Pollak, E. *J. Chem. Phys.* 1986, *85*, 865.

(129) Rosenthal, S. J.; Xie, X.; Du, M.; Fleming G. R. *J. Chem. Phys.* 1991, *95*, 4715.

(130) (a) Maroncelli, M.; Fleming, G. R. *J. Chem. Phys.* 1988, *89*, 5044. (b) Maroncelli, M.; MacInnis, J.; Fleming, G. R. *Science* 1989, *243*, 1674. (c) Maroncelli, M. *J. Chem. Phys.* 1991, *94*, 2084.

(131) Fleming, G.; Wolynes, P. G. *Phys. Today* 1990, *5*, 36.

(132) Cho, M.; Rosenthal, S. J.; Scherer, N. F.; Ziegler, L. D.; Fleming, G. *J. Chem. Phys.* 1992, *96*, 5033.

(133) Hirata, Y.; Murata, N.; Tanioka, Y.; Mataga, N. *J. Phys. Chem.* 1989, *93*, 4527.

(134) (a) Hirata, Y.; Mataga, N. *J. Phys. Chem.* 1990, *94*, 8503. (b) Wang, Y.; Crawford, M. K.; Mcauliffe, M. J.; Eisenthal, K. B. *Chem. Phys. Lett.* 1980, *74*, 160. (c) Chase, W. J.; Hunt, J. W. *J. Phys. Chem.* 1975, *79*, 2835.

(135) Bader, J. S.; Chandler, D. *Chem. Phys. Lett.* 1989, *157*, 501.

(136) Pratt, L. R. *Ann. Rev. Phys. Chem.* 1985, *36*, 433.

(137) Rossky, P. J. *Ann. Rev. Phys. Chem.* 1985, *36*, 321.

(138) Frank, H. S.; Evans, M. W. *J. Chem. Phys.* 1945, *13*, 507.

(139) Franks, F. *Water-A comprehensive Treatise*; Plenum: New York, 1973; Vol. 2, Chapter 5.

(140) Ben-Naim, A. *Hydrophobic Interactions*; Plenum: London, 1980.

(141) Tanford, P. *The Hydrophobic Effect*; Wiley: New York, 1980.

(142) Kauzmann, W. *Adv. Protein Chem.* 1959, *14*, 1.

(143) McMillan, W. G.; Mayer, J. E. *J. Chem. Phys.* 1945, *13*, 276.

(144) (a) Friedman, H. L. *J. Solution Chem.* 1973, *1*, 387; 413; 418.

(145) (a) Pierotti, R. A. *J. Phys. Chem.* 1963, *67*, 1840. (b) Pierotti, R. A. *J. Phys. Chem.* 1965, *69*, 281.

(146) Reiss, H. *Adv. Chem. Phys.* 1965, *9*, 1.

(147) Postma, J. P. M.; Berendsen, H. J. C.; Haak, J. R. *Faraday Symp. Chem. Soc.* 1982, *17*, 55.

(148) (a) Stillinger, F. H. *J. Solution Chem.* 1973, *2*, 141. (b) Irisa, M.; Nakamura, H.; Hirata, F. *Chem. Phys. Lett.* 1993, *207*, 430.

(149) Pratt, L. R.; Chandler, D. *J. Chem. Phys.* 1977, *67*, 3683.

(150) Pratt, L. R.; Chandler, D. *J. Chem. Phys.* 1980, *73*, 3434.

(151) Pratt, L. R.; Chandler, D. *J. Chem. Phys.* 1980, *73*, 3430.

(152) (a) Tani, A. *Mol. Phys.* 1983, *48*, 1229. (b) Tani, A. *Mol. Phys.* 1984, *51*, 161.

(153) Widom, B. *J. Chem. Phys.* 1963, *39*, 2808.

(154) Straatsma, T. P.; Berendsen, H. J. C.; Postma, J. P. M. *J. Chem. Phys.* 1986, *85*, 6720.

(155) (a) Pearlmann, D. A.; Kollman, P. A. *J. Chem. Phys.* 1989, *90*, 2460. (b) Pearlmann, D. A.; Kollman, P. A. *J. Chem. Phys.* 1989, *91*, 7831.

(156) Cracknell, R. F.; Nicholson, D.; Parsonage, N. G.; Ewans, H. *Mol. Phys.* 1990, *71*, 931.

(157) Swope, W. C.; Andersen, H. C. *J. Phys. Chem.* 1984, *88*, 6548.

(158) Hill, T. L. *Statistical Mechanics*; McGraw-Hill: New York, 1956.

(159) Guillot, B.; Guissani, Y.; Bratos, S. *J. Chem. Phys.* 1991, *95*, 3643.

(160) Jorgensen, W. L.; Madura, J. D. *J. Am. Chem. Soc.* 1983, *105*, 1407.

(161) (a) Pangali, C.; Rao, M.; Berne, B. J. *J. Chem. Phys.* 1979, *71*, 2975. (b) Ravishanker, C.; Mezei, M.; Beverridge, D. L. *Faraday Symp. Chem. Soc.* 1982, *17*, 97. (c) Swaminathan, S.; Beveridge, D. L. *J. Am. Chem. Soc.* 1979, *101*, 5932.

(162) (a) Geiger, A.; Rahman, A.; Stillinger, F. H. *J. Chem. Phys.* 1979, *70*, 263. (b) Rapaport, D. C.; Scheraga, H. A. *J. Phys. Chem.* 1982, *86*, 873. (c) Watanabe, K.; Andersen, H. C. *J. Phys. Chem.* 1986, *90*, 795. (d) Zichi, D. A.; Rossky, P. J. *J. Chem. Phys.* 1986, *84*, 2814.

(163) (a) Pratt, L. R.; Haan, S. W. *J. Chem. Phys.* 1981, *74*, 1864. (b) Pratt, L. R.; Haan, S. W. *J. Chem. Phys.* 1981, *74*, 1873.

(164) Tanaka, H.; Gubbins, K. E. *J. Chem. Phys.* 1992, *97*, 2626.

(165) (a) Jorgensen, W. L. *J. Chem. Phys.* 1982, *77*, 5757. (b) Rosenberg, R. O.; Mikkilineni, R.; Berne, B. J. *J. Am. Chem. Soc.* 1982, *104*, 7647.

(166) Ben-Naim, A. *J. Chem. Phys.* 1989, *90*, 7412.

(167) Tanaka, H.; Nakanishi, K. *J. Chem. Phys.* 1991, *95*, 3719.